AD-A154 776 QUALITATIVE ANALYSIS OF SIGN-BIT PROCESSING(U) COLORADO SCHOOL OF MINES GOLDEN CENTER FOR WAVE PHENOMENA I LEROUX 30 APR 85 CWP-028 N00014-84-K-0049 1/2

UNCLASSIFIED F/G 9/2 NL

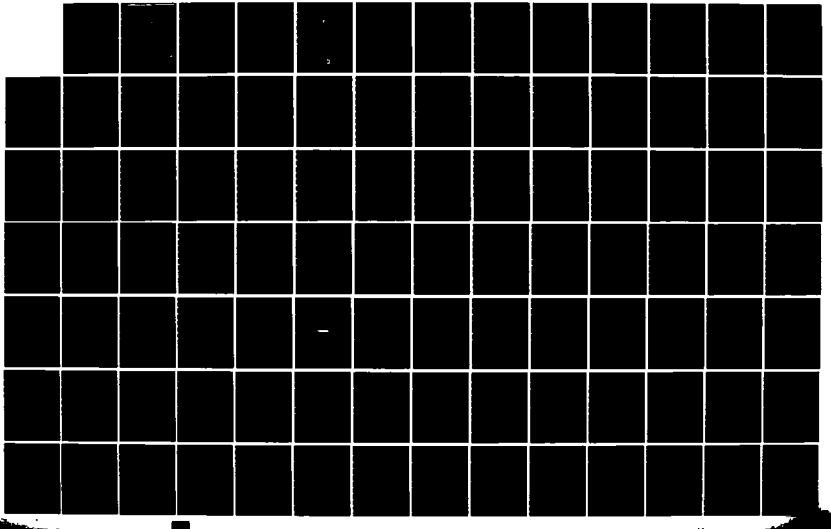

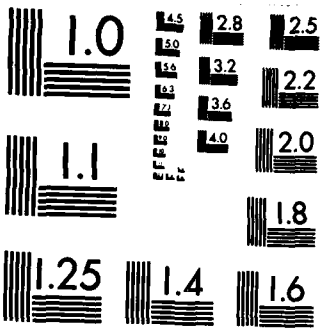

(2)

CSM

Qualitative analysis of sign-bit processing

by

Isabelle Leroux

Partially supported by the Selected Research Opportunities Program of the Office of Naval research

Colorado School of Mines
Golden, Colorado 80401

Center for Wave Phenomena
Department of Mathematics
303/273-3557

85 5 16 031

UNCLASSIFIED

SECURITY CLASSIFICATION OF THIS PAGE (When Data Entered) A154 776

REPORT DOCUMENTATION PAGE		READ INSTRUCTIONS BEFORE COMPLETING FORM
1. REPORT NUMBER CWP-028	2. GOVT ACCESSION NO.	3. RECIPIENT'S CATALOG NUMBER
4. TITLE (and Subtitle) Qualitative analysis of sign-bit processing		5. TYPE OF REPORT & PERIOD COVERED Technical 6. PERFORMING ORG. REPORT NUMBER
7. AUTHOR(s) Isabelle Leroux		8. CONTRACT OR GRANT NUMBER(s) N00014-84-K-0049
9. PERFORMING ORGANIZATION NAME AND ADDRESS Center for Wave Phenomena Department of Mathematics Colorado School of Mines, Golden, CO 80401		10. PROGRAM ELEMENT, PROJECT, TASK AREA & WORK UNIT NUMBERS NR SRO-159/84APR20(411)
11. CONTROLLING OFFICE NAME AND ADDRESS Office of Naval Research Arlington, VA 22217		12. REPORT DATE 04/30/85 13. NUMBER OF PAGES 115
14. MONITORING AGENCY NAME & ADDRESS(if different from Controlling Office)		15. SECURITY CLASS. (of this report) 15a. DECLASSIFICATION/DOWNGRADING SCHEDULE

16. DISTRIBUTION STATEMENT (of this Report)

This document has been approved for public release and sale; its distribution is unlimited.

17. DISTRIBUTION STATEMENT (of the abstract entered in Block 20, if different from Report)

18. SUPPLEMENTARY NOTES

19. KEY WORDS (Continue on reverse side if necessary and identify by block number)

Born inversion method, location of the reflectors, velocity computation, noise-to-signal ratio, sign-bit

20. ABSTRACT (Continue on reverse side if necessary and identify by block number)

see reverse side

DD FORM 1 JAN 73 1473 EDITION OF 1 NOV 65 IS OBSOLETE
S/N 0102-014-6601 |

SECURITY CLASSIFICATION OF THIS PAGE (When Data Entered)

ABSTRACT

This paper discusses the sign-bit processing in the Born inversion method. It shows on basic examples that in the absence of relative true amplitude, the Born inversion algorithm written by Bleistein-Cohen still provides an image of the subsurface. It implies that all the essential information provided by a wave train is contained in the phase only. Sign-bit digital recording means that only the sign of the true amplitude signal is recorded with one bit. In conventional seismic recording, 16 to 32 binary bits per sample point are recorded. The economic advantages of sign-bit acquisition are immediately obvious. Complete amplitude recovery comparable to full gain recording can be achieved by correct application of sign-bit techniques.

CWP-028

Qualitative analysis of sign-bit processing

by

Isabelle Leroux

Partially supported by the Selected Research Opportunities Program of the Office of Naval research

Accession For	
NTIS GRA&I	☒
DTIC TAB	☐
Unannounced	☐
Justification	
By	
Distribution/	
Availability Codes	
Dist	Avail and/or Special
A/1	

Center for Wave Phenomena
Department of mathematics
Colorado School of Mines
Golden, Colorado 80401
Phone: (303) 273-3557

ACKNOWLEDGEMENTS

I am very grateful to my thesis advisor, Dr. Norman Bleistein, for his guidance in every phase of this study, for providing encouragement and support throughout my study.

Sincere thanks are due to Dr. Boes for his financial support for my studies.

Special appreciation also goes to Colorado School of Mines for the use of their computer systems.

TABLE OF CONTENTS

LIST OF FIGURES

ALGORITHM

OF THE

MODIFIED PROGRAM GEO2D

If IENTER = 1, then :

creation of time traces;

adding noise if desired;

If IENTER $\leq$ 2, then :

filtering the time section;

replacing the amplitude by one or two bits;

filtering the new time section;

If IENTER $\leq$ 3, then :

performing the computation of the jump in velocity.

Table II.2

GEO2D.

This algorithm is directed by the variable IENTER which allows the user entering the program at different level in the code depending on whether the user is inputting data from a data tape or generating test data in line.

For IENTER=1 the execution begins from the creation of time traces, that is the scattered wave function will be created. The wave function due to the noise is added to this wave accordingly to the noise-to-signal ratio given in the data. The subroutine NOISE implements that function.

For IENTER$\leq$2 the wave function will be filtered to provide high-frequency data to the remaining code. This filtering part includes other operations requested by the formula. The modifications needed to generate sign-bit data are done within the main program, after the filtering process (see the algorithm table II.2).

The inserted code generates a function with sign-bit amplitude from the wave function created previously if IENTER=1, or gathered on the field. That is the initial scattered wave is translated in the Fourier domain, to be filtered with the same filter as before. This bandlimited signal is then studied in the time domain and sign-bit processing will be applied. These high frequency data will be replaced by sign-bits according to the sign of the amplitudes of the function if two numbers, -1 and +1, are used, or to the value of the amplitude if three numbers, -1, 0 and +1, are used , as follows:

ALGORITHM

OF THE

ORIGINAL PROGRAM GEO2D

If IENTER = 1, then :

creation of time traces;

adding noise if desired;

If IENTER $\leq$ 2, then :

filtering the time section;

If IENTER $\leq$ 3, then :

performing the computation of the jump of velocity.

Table II.1

II. MEANS USED FOR THE STUDY.

A. The computer program GEO2D.

The program GEO2D computes $\alpha(x,z)$ for the 2.5 dimensional model. That is, we consider the wave spreading in three dimensions but we compute the integral on the geophone array in two dimensions under the assumption that α is independent of y.

For the gradient of α, called β, we get the processing formula in 2.5 dimensions:

$$\beta(x,z) \sim \frac{16\pi z}{\sqrt{c}} \int \frac{d^2\xi}{R^{3/2}} [Re - Im] \int df \cdot \sqrt{f} \cdot F(f) \cdot \exp(-2\pi i f \cdot 2R/c) \cdot \int_0^{+\infty} dt \cdot t \cdot U_s(\xi,t) \cdot \exp(2\pi i f t) \qquad (2)$$

where: c, reference speed;

(x,z) is a field point

R, distance form the field point to the observation point;

f, frequency;

F(f), filtering function;

ξ, geophone location;

$U_s(\xi,t)$, scattered wave;

The chart in table II.1 is an algorithm of the original program

function of the sound-speed perturbation α and derive reflector maps. Computer plots are presented to illustrate the outputs of these computations and to analyze the effects of sign-bit processing.

$$\frac{1}{v^2} = \frac{1}{c^2}\,[1 + \alpha(x,y,z)] \qquad (1)$$

where: - $(x,y,z) = (\underline{x},z)$ is a field point;

- v is the velocity at the field point (x,y,z);

- c is the reference velocity;

- $\alpha(x,y,z)$ is the perturbation at the field point.

However field data is not full bandwidth data and it cannot be simply processed to yield a solution for α. Instead a partial inversion consistent with the high frequency characterization of the field data is carried out.

The Fourier transform of a function contains information about the trend of a function at the low frequencies or small values of the wave number and information about discontinuities at high frequencies or large values of the wave number. Thus the solution formula is modified to process only for the discontinuities in $\alpha(x,y,z)$, that is, the reflectors in the subsurface will be located by the peak amplitudes of the gradient function of α, called β in the following discussions.

The wave field received at the geophones is the required data to compute the function β. The latter behave like a bandlimited delta function across each reflector. For true amplitude data, the peak amplitude data at each reflector is in known proportion to the reflection strength.

The true amplitude data and the sign-bit data are processed through the Born inversion algorithm to compute the magnitude of the gradient

The purpose of this paper is to show that in the absence of relative true amplitude the velocity inversion algorithm still provides an image of the reflecting subsurfaces as it was remarked in the report of Bleistein, and Cohen (1984). Several noise-to-signal ratios are introduced in the scattered wave and the noise effects are analyzed in the results of the Born inversion algorithm. Furthermore, the reflection strength is compared with the jump in velocity given in the data for each example that will have been processed in the Born inversion algorithm.

C. Method of approach.

The inverse problem is written for the acoustic wave equation. The method was written for a perturbation from a reference sound-speed. A nonlinear integral equation, involving the product of the unknown perturbation and the unknown wave field in the earth was derived in Cohen and Bleistein (1979) and is also described in Bleistein (1984). The solution formula requires full bandwidth data which is not available in the seismic experiment. In fact the data can be characterized as high frequency data with respect to most of the length scales of the seismic experiment.

The integration formula for the inversion uses Fourier transforms to yield the perturbation function α defined by:

The papers which are referenced in this literature review discussed sign-bit techniques to store the seismic data. These data were then processed through typical geophysical programs. The results were analyzed to check how they report information about the subsurface, especially in noisy environments. This paper will analyze in the same way the results of a new mathematical interpretation of the seismic data. The major additional feature of this new method is that for true amplitude data, the amplitude of the output is in known relation to the reflection strength. Thus, we can check amplitude accuracy of sign-bit processing as well as image accuracy.

B.Purpose and objectives of study.

We use here a mathematical approach to seismic inversion presented by Cohen and Bleistein (1979) with computer implementation in Bleistein and Cohen (1984). The authors used the Born approximation and asymtotic analysis to derive an algorithm to process seismic data and recover both the location of the reflectors in the earth and to estimate the reflection strength at each reflector. This approach builds the Born inversion algorithm. An asymptotic analysis of the output of this algorithm was made in the same report. One of the conclusions drawn from this analysis is that errors in amplitude in the input will degrade the estimate of reflection strength, however they will not affect estimates of the location of the reflector.

acceptable;

(ii) high compression of the data, more field processing controls are possible;

(iii) true amplitude relations are maintained; and the procedure is tailormade for Vibroseis.

The principal disadvantages stated by the authors are:

(i) the method is limited to Vibroseis;

(ii) a heavy duty 60Hz single phase power plant is a possible source of coherent noise;

(iii) a bad spread cable or array terminal can cause a great loss of data;

(iv) the dynamic range is limited;

(v) a higher caliber field personnel is needed.

Then Gimlin and Smith (1977) and Smith and Gimlin (1977) presented two additional papers related to sign-bit studies.

An analysis of sign-bit recording for high and low noise environments was made by Shirley et al. (1983) for the SEG meeting in Las Vegas, 1983. This approach to sign-bit results in a unified description of the low noise-to-signal and high noise-to-signal cases. A single expression that is valid for all random noise distributions shows the relationship between input coherent energy, input random noise, and output expectation.

Yuan Cheng Lee(1984) studied the amplitude recovery with sign-bit data. Several examples including different noise-to-signal ratios were run and the effects of the noise in the amplitude recovery were analyzed.

conventionnally. Examples of actual noisy environment conditions are shown together with the effect of superimposing that noise on simulated Vibroseis data and processing it with conventional and sign-bit recordings. They simulated several types of variable noise on the computer and noted that they have minimal effect on sign-bit data. In the presence of high amplitude background noise, such as could be expected in populated areas, on windy days, near the surf, or in stormy seas, seismograms resulting from sign-bit data are shown to be significantly superior to those from conventional floating point recording systems. Thus, in a typical noisy environment the system recording sign-bit only should require significantly fewer memory modules and consequently reduced costs to acquire data comparable or superior to those from conventional systems.

Schoellhorn et al. (1975) simulated sign-bit summing in vibroseis data acquisition on the computer. A variety of multiple arrivals with differing amplitudes were evaluated, these showed the expected effects of amplitude ratio loss, spectral loss when the noise-to-signal ratio is less than one, and high impulse noise immunity. However, field data comparisons of full range and sign-bit summing showed only minor differences in the final stacked sections.

An evaluation of sign bit seismic recording and its impact on processing and interpretation was made by Alihilali et al. (1975). They evaluated the advantages and disadvantages of sign-bit recording. Some of the primary advantages claimed by the authors are:

(i) smaller, simpler spread cables and single element geophones are

I. INTRODUCTION

Sign-bit data recording has interested the seismic exploration industry for many years because it provides an easy way to greatly decrease the number of channels in a data acquisition system. Sign-bit digital recording means that only the sign of the analog signal is recorded with one bit. In conventional seismic recording 16 to 32 binary bits are necessary for each sample point. So the economic advantages of sign-bit recording are obvious. It is necessary to check that the results obtained from usual seismic processings are valid and still provide good information.

A. Literature review.

Numerous published papers deal with the data storage using signed bits and with the amplitude recovery from the information carried by these data on the subsurfaces. Discussions of sign-bit data recording in geophysical literature consist mainly of abstracts of papers at international SEG meetings. The first paper was presented by Fort et al. (1973). Four papers were presented in 1975, namely, Fort et al. (1975), Martin et al. (1975), Schoellhorn and Neale. (1975), and Alihilali et al. (1975), Martin et al. (1975) claimed that the noise burst problems with Vibroseis are minimized by only using the sign-bit. Computer simulation shows that if only sign-bit data is used, reflection quality is improved over that obtained

ABSTRACT

This paper discusses the sign-bit processing in the Born inversion method. It shows on basic examples that in the absence of relative true amplitude, the Born inversion algorithm written by Bleistein-Cohen still provides an image of the subsurface. It implies that all the essential information provided by a wave train is contained in the phase only. Sign-bit digital recording means that only the sign of the true amplitude signal is recorded with one bit. In conventional seismic recording, 16 to 32 binary bits per sample point are recorded. The economic advantages of sign-bit acquisition are immediately obvious. Complete amplitude recovery comparable to full gain recording can be achieved by correct application of sign-bit techniques.

→ See p. 1 -

LIST OF TABLES

1)- When the amplitude is positive, it is replaced by +1. If it is negative, its value becomes -1.

or

2)- The maximum amplitude is stored in UMAX. When the sample value is less than a certain percentage (stored in the variable PER) of UMAX, it is replaced by 0. If this value is larger, then the amplitude replacement follows 1) above.

The new signal or succession of bits is then processed through the same filtering algorithm used for the initial scattered wave, to eliminate low and high frequencies which might have been introduced in the sign-bit processing .

To complete the formula an integration loop (ξ in eq. 2) is carried out over a set of processed traces for each point in the region of interest in the field. The data delimits this region where it is possible to image the interface or reflector or discontinuity in the earth. For each field point (x, z), the previous function is divided by $R^{3/2}$ and multiplied by z. The results of the integration are scaled by a factor SCALE, to generate β, which is then an estimation of the jump in velocity.

The plot of this function enables us to study and follow the discontinuities in the earth model which reflected the initial wave.

B. Description of the data required by the program GEO2D.

The data required to execute the program GEO2D is described in the following sections.

The data is entered in free format:

RECORD #1

IENTER: 1 = SYNTHETIC DATA GENERATION.

2 = READ FROM TAPE7 OF DECONVOLVED TRACES.

3 = READ FROM TAPE8 OF PROCESSED TRACES.

RECORD #2

TMIN: BEGINNING OF TIME RECORD MEASURED FROM ENTRY TIME OF SOURCE PEAK.

TMAX: END OF TIME RECORD.

DT: SAMPLING RATE.

NFFT: SIZE OF FFT.

RECORD #3

FMIN0: FREQUENCY AT WHICH TAPER FILTER BEGINS.

FMIN1: FREQUENCY AT WHICH TAPER REACHES ONE AT LOW END.

FMAX1: FREQUENCY AT WHICH TAPER FILTER ENDS.

RECORD #4

NGEO: NUMBER OF GEOPHONES (TRACES).

DXSI: GEOPHONE SPACING.

RECORD #5

C: REFERENCE SPEED.

RECORD #6

ZMIN: SHALLOWEST Z (.GE.0) TO BE PROCESSED.

ZMAX: DEEPEST Z TO BE PROCESSED.

DZ: Z-SPACING DESIRED.

RECORD #7

XMIN: LEFTMOST X (.GE.0) TO BE PROCESSED.

XMAX: RIGHTMOST X TO BE PROCESSED.

DX: X-SPACING DESIRED.

RECORD #8

NGROUP: NUMBER OF GEOPHONES TO BE HELD IN CORE.

RECORD #9

MKPRNT: TRUE FOR PRINTOUT OF VELOCITY PROFILE.

MKTAPE: TRUE FOR MAKING VELOCITY PROFILE TAPE.

MKPLOT: TRUE FOR MAKING VELOCITY PROFILE PLOT.

RECORD #10

THETS: TILT ANGLE OF SYNTHETIC DATA PLANES.

NPLN: NUMBER OF SYNTHETIC DATA PLANES.

NOISIG: NOISE TO SIGNAL RATIO.

RECORD #11

CS(I): SYNTHETIC DATA SPEED ARRAY.

RECORD #12

ZS(I): SYNTHETIC DATA DEPTHS OF PLANES AT X=0.

RECORD #13

GOGO: SET TRUE TO CONTINUE RUN WITH BAD DATA.

III. SEVERAL EXAMPLES.

In every example the synthetic time section is created for a subscribed subsurface structure; it is represented on the first plot of each following section. Then these traces are processed through the first part of the Born inversion algorithm. This process is illustrated on the plots named "PROCESSED TIME SECTION". On the synthetic time sections and on the processed time sections, the reflectors are located in time; that is the scattered functions peak at the travel time necessary for the wave to go from the geophone array to the reflectors. After the true amplitude data have been processed, the scattered wave undulates only around the interface location. On the contrary, after sign-bit data processing the scattered wave is undulating everywhere on the time section and it is more difficult to locate in time the reflectors. A reason is that after having been filtered the synthetic traces were replaced by +1 or -1 all along the time section so that the side lobes become as important as the main lobe.

Then the integration loop completes the velocity computation. At the center of the span array of the geophones, there is just enough spread to include all geophones that could contribute to the answer, that is to the amplitude of the velocity. A number of 81 geophones was chosen to get a good approximation of the velocity. The resulting function peaks at the interface locations, with true amplitude data as well as with sign-bit data. For each example, the amplitude of the resulting function will be

checked at the middle of the span array. The results will be discussed more precisely for each example.

A. The discontinuity is a single horizontal plane.

The data set for this example is given in Appendix A. The plane is located 2000 ft. below the surface. The theoretical jump in velocity due to this discontinuity in the earth is 500 ft./sec. The plots III.A.1 illustrates these data.

The results of the filtering process are shown on the plot III.A.2 when the true amplitude data were processed and on the plot III.A.4 when the sign-bit amplitude data were processed.

The plots on Figures III.A.3 and III.A.5 show both results of the velocity computation, the former with true amplitude and the latter with sign-bit amplitude. Both calculations locate the plane discontinuity in the earth at the same depth. The numerical results are shown in table III.A. The jump in velocity will be read at the abscissa 1000ft from the left and at the depth 2000ft. The error in amplitude is computed from the difference between the jump in velocity given in the data, 500ft/sec., and the jump in velocity read in the results of the velocity computation.

OUTPUT OF THE VELOCITY COMPUTATION
WITH ONE HORIZONTAL REFLECTOR, NO NOISE

	with true amplitude data	with sign-bit amplitude data
Depth (feet) of the reflector	2000.	2000.
Jump (ft/sec) at X=1000,Z=2000	485.515	459.31
error in amplitude (%)	-2.9	-8.

Table III.A

B. The discontinuity is an inclined plane.

The data set for this example is given in Appendix B, where the angle THETS has been replaced by 10^{o}, and is illustrated on the plot III.B.1. Before the velocity computation the filtering process is applied on the true amplitude data giving the time section illustrated on the Figure III.B.2. After having applied the sign-bit processing on the true amplitude data the same filtering process is applied on the sign-bit data giving the results viewed on the Figure III.B.4.

The outputs of the velocity computation with true amplitude data (Figure III.B.3) and with sign-bit data (Figure III.B.5) both accurately locate the interface. The numerical results are displayed in the table III.B, the error is calculated from a prescribed jump in velocity which is 500ft/sec.

C. Example with two horizontal interfaces.

The data set for this example is given in Appendix C and is illustrated on Figure III.C.1. A first filter is applied to the synthetic time section and the processed time section is illustrated on the Figure III.C.2. In a second run the sign-bit process is applied to the synthetic time section to create sign-bit data which are then processed through the same filter and this second processed time section is illustrated on the

Figure III.C.5.

OUTPUT OF THE VELOCITY COMPUTATION
WITH ONE REFLECTOR, TILTED, NO NOISE

	with true amplitude data	with sign-bit amplitude data
Depth (feet) of the reflector	2000.	2000.
jump (feet/sec) at X=1300,Z=1770	464.795	440.595
error in amplitude (%)	-6.64	-11.8

Table III.B

The outputs of the velocity computation in both runs are illustrated on the Figure III.C.3 and Figure III.C.6. They locate the interfaces at the same depths. After both computations the upper interface is at the right location (1700ft) and the deeper interface is mislocated: its depth is 2250ft instead of 2300ft. After having processed these outputs in the postprocessing algorithm POSTPP, which implements the refinements to the linear velocity inversion theory (Hagin and Cohen, 1984), both reflectors are located approximately at the right depths (see Figures III.C.4 and III.C.7). The numerical results are displayed in the table III.C.

D. Example with 2 tilted parallel interfaces.

The data set for this example is given in Appendix C, where the angle THETS has been replaced by 10^{o}; both interfaces are inclined to make 10^{o} with the horizontal. The scattered wave field is on Figure III.D.1. We notice that the amplitude of the wave peaks shaping the deepest interface is smaller than the one locating the upper subsurface.

In the processed time section (Figure III.D.2) it is more difficult to locate the deeper interface than the upper one. The time section with sign-bit amplitude is processed through the first part of the Born inversion algorithm, the results are represented on the plot on Figure III.D.4.

OUTPUT OF THE VELOCITY COMPUTATION
WITH 2 HORIZONTAL REFLECTORS, NO NOISE

	with true amplitude data		with sign-bit amplitude data	
	without postprocessing	after postprocessing	without postprocessing	after postprocessing
Depth (feet) of the:				
-reflector 1	1700.	1711.	1700.	1711.
-reflector 2	2250.	2320.	2250.	2320.
a (feet/sec)				
-reflector 1				
at (1000,1700)	498.318		392.393	
at (1000,1711)		561.11		440.52
-reflector 2				
at (1000,2250)	423.738		407.271	
at (1078,2320)		548.13		
at (1027,2320)				518.80
error in amplitude (%)				
-reflector 1	-0.52	+12.	-21.5	-11.9
-reflector 2	-15.25	+ 9.6	-18.5	+ 3.8

TABLE III.C

The outputs of the velocity computation with true amplitude data (Figure III.D.3) and with sign-bit amplitude data (Figure III.D.5) locate the interfaces clearly at the same depths. The numerical results are shown in the table III.D. The error is calculated after comparison of the computed jump with 500ft/sec. for the upper reflector and with 200ft/sec. for the lower interface.

The accuracy of the computed jump in velocity depends on the distance between reflectors. Examples were also run with 300ft and with 200ft between the subsurfaces, showing that the computed jumps in velocity are interrelated: when the distance gets smaller, the error in amplitude gets smaller for the lowest reflector and the error for the uppest one gets larger.

Otherwise the subsurfaces were located with the same characteristics as in the previous example III.D, that is, the velocity function peaks at the right depth for the upper subsurface, and about 20ft above the prescribed depth for the deepest reflector.

The above remarks are for true amplitude data processing and for sign-bit data processing.

OUTPUT OF THE VELOCITY COMPUTATION
WITH 2 REFLECTORS, TILTED, NO NOISE

	with true amplitude data	with sign-bit amplitude data
Depth (feet) at X=0ft of the:		
-reflector 1	1900.	1900.
-reflector 2	2360.	2350.
Jump (ft/sec) -reflector 1 at (1000, 1720)	507.782	433.553
-reflector 2 at (1000, 2180)	202.642	425.228
error in amplitude (%)		
-reflector 1	+1.56	-13.3
-reflector 2	+0.52	+45.

Table III.D

E.The scattering subsurface is an arc of circle.

The subsurface is represented in Figure III.E.1. The speed is c_o above the arc of circle and c_+ below it. The radius of the circle is a=3000ft and its highest point is located at the depth h=1000ft below the center of the array of geophones.

Using the data given in Appendix D, the synthetic time section (Figure III.E.1) is created using the following formula which is derived in the paper: Kirchhoff field from a circular cylinder (Bleistein, 1984), using the Two-and-one half dimensional in-plane wave propagation (Bleistein, 1984), it is implemented in the subroutine TRACIR of the program GEO2D.

$$U_S(\omega,\xi) \sim \sqrt{\frac{a}{b}} \cdot \frac{R_n \cdot \exp(2i\omega(d-a)/c_o)}{8\pi(d-a)} \qquad (3)$$

where:

- ω is the pulsation;
- $\underline{\xi}=(\xi,0)$ is the location on the geophone array;
- R_n is the normal reflection coefficient;
- $d = (\xi^2 + (a+h)^2)^{1/2}$;
- $4c(2(d-a))$ is the geometrical spreading over the two way travel path from $\underline{\xi}$ to C and back to $\underline{\xi}$, in the abscence of curvature effects of the reflector.
- $(a/d)^{1/2}$ is the geometrical spreading due to a circular reflector of radius a at depth h.
- $2(d-a)/c_o$ is the two way travel time.

The processed time sections with true amplitude data and with sign-bit

data are represented on Figure III.E.2 and on Figure III.E.4 respectively.

The output of the velocity computation with true amplitude data locates the subsurface at the right depth (Figure III.E.3). The profile computed with sign-bit amplitude data (Figure III.E.5) locates the interface at the same depth. The numerical results are displayed in the table III.E.

peaks everywhere with large amplitudes.

From this chapter IV, the following conclusions can be drawn:

1. When the noise-to-signal ratio is less than or around 1, the reflectors are easily located at the right depth with sign-bit data as well as with true amplitude data.

2. When the noise-to-signal ratio is much larger than 1, it is more difficult to locate the reflectors on the plot representing the output of the velocity computation. This output does not peak at the right location of the interface. The error in depth increases as the noise-to-signal ratio gets larger. The same conclusion can be drawn with true amplitude data and with sign-bit data.

3. The Figure IV.C.3 illustrates the curves of the errors in jump in velocity from true amplitude data processing and from sign-bit data processing versus the noise-to-signal ratios. Both curves have the same trend. When the noise-to-signal ratio gets large the errors from sign-bit data processing are smaller than those from true amplitude data processing, but when N/S is small the former are bigger than the latter.

4. When two bits are used to store the data, the reflector is easier located, that is the resulting function less ondulates than when sign-bit was used. The accuracy depends on the threshold.

5. Not filtering the sign-bit data gives rise to large errors in the velocity computation.

OUTPUT OF THE VELOCITY COMPUTATION
WITH ONE HORIZONTAL REFLECTOR, N/S=0.5
WITH THRESHOLD=0.26

	with sign-bit data	with threshold
depth in feet of the reflector	2000.	2000.
jump in feet/sec. at X=1000ft,Z=2000ft	368.513	315.582
error in amplitude (%)	-26.3	-36.9

Table IV.B.3

OUTPUT OF THE VELOCITY COMPUTATION
WITH ONE HORIZONTAL REFLECTOR, N/S=0.5
WITH THRESHOLD=0.1

	with sign-bit data	with threshold
depth in feet of the reflector	2000.	2000.
jump in feet/sec. at X=1000ft, Z=2000ft	368.513	359.41
error in amplitude (%)	-26.3	-28.1

Table IV.B.2

processing with a percentage equal to 10% of the maximum signal amplitude. The numerical results are displayed in the table IV.B.2.

The same configuration is given with a percentage PER equal to 26%. The synthetic time section is represented on Figure IV.A2.1. The processed time sections with sign-bit data and with threshold, on Figure IV.A2.3 and Figure IV.B.5 respectively, are identically complex. The outputs of the velocity computation are represented on Figure IV.A2.4 when sign-bit were used and on Figure IV.B.6 when threshold was used. The amplitudes of the smiles are smaller in the latter plot than in the former one. The noise influence has been slightly eliminated after threshold processing with a percentage equal to 26% of the maximum signal amplitude. The numerical results are displayed in the table IV.B.3.

C. The output resulting from noise added to sign-bit data is not filtered.

In this section, we add a noise with N/S=0.5 to the sign-bit data. Then the resulting function is processed through the velocity computation, without having previously been filtered. The plots IV.C.1 and IV.C.2 illustrate the processed time section and the output of the velocity computation respectively. On the former it is impossible to locate in time the reflector. On the latter, the velocity function

OUTPUT OF THE VELOCITY COMPUTATION
WITH ONE HORIZONTAL REFLECTOR, N/S=0.5
WITH THRESHOLD=.05

	with sign-bit data	with threshold
depth in feet of the reflector	2000.	2000.
jump in feet/sec. at X=1000ft,Z=2000ft	368.513	370.797
error in amplitude (%)	-26.3	-25.84

Table IV.B.1

variable PER in the data for the program GEO2D. When the amplitudes are below this limit they will be replaced by zero.

A configuration is given in the data in Appendix B with a percentage PER equal to 5%. The synthetic time section is represented on Figure III.A.1. In this section, only the computations using sign-bit processing are dicussed. The processed time sections with sign-bit data and with two bits data, on Figure IV.A2.3 and Figure IV.B.1 respectively, are identically complex. The outputs of the velocity computation are represented on Figure IV.A2.4 when one bit was used and on Figure IV.B.2 when two bits were used. The amplitudes of the smiles are smaller in the latter plot than in the former one.

The noise influence has been slightly eliminated after threshold processing with a percentage equal to 5% of the maximum signal amplitude. The numerical results are displayed in the table IV.B.1.

The same configuration is given with a percentage PER equal to 10%. The synthetic time section is represented on Figure IV.A2.1. The processed time sections with sign-bit data and with two bits data, on Figure IV.A2.3 and Figure IV.B.3 respectively, are identically complex. The outputs of the velocity computation are represented on Figure IV.A2.4 when two bits were used and on Figure IV.B.4 when two bits were used. The amplitudes of the smiles are smaller in the latter plot than in the former one.

The noise influence has been slightly eliminated after two bits

OUTPUT OF THE VELOCITY COMPUTATION
WITH ONE HORIZONTAL REFLECTOR, N/S=25.6

	with true amplitude data	with sign-bit amplitude data
depth in feet of the reflector	1980.	1980.
jump in feet/sec. at X=1000ft,Z=1980ft	663.454	600.015
error in amplitude (%)	+32.7	+20.

Table IV.A4

sections and the processed time sections are very messy: it is more difficult than before to distinguish the delta amplitude corresponding to the subsurface (see Figures IV.A4.1, IV.A4.2 and IV.A4.4). After the velocity computation, the resulting function peaks at several depths with about the same amplitude at each of them. Thus it is difficult to locate the reflector after true amplitude data processing as well as after sign-bit data processing (see Figures IV.A4.3 and IV.A4.5). The numerical results are displayed in table IV.A4.

the results of executions with bigger noise-to-signal ratios show larger larger errors in the location of the reflector as well as in the amplitude of the jump in velocity.

B. Using two bits to replace the amplitude.

Before entering the sign-bit processing, the created signal has definite amplitudes everywhere in the time interval, most of them are smaller than the trigger value locating the subsurface. However all of them will be replaced by +1 and -1 as well as the maximum value. That is why the processed time sections and the outputs of the velocity computation are more complicated. That can make difficult the delimitation of the interfaces on the plots, among the smiles .

To eliminate this problem, the amplitudes of the scattered wave function will be replaced by sign-bit only when these values are above a percentage of the maximum amplitude: this percentage is given by the

OUTPUT OF THE VELOCITY COMPUTATION
WITH ONE HORIZONTAL REFLECTOR, N/S=1.

	with true amplitude data	with sign-bit amplitude data
depth in feet of the reflector	2000.	2000.
jump in feet/sec. at X=1000ft,Z=2000ft	500.235	359.598
error in amplitude (%)	-0.	-28.1

Table IV.A3

OUTPUT OF THE VELOCITY COMPUTATION
WITH ONE HORIZONTAL REFLECTOR, N/S=0.5

	with true amplitude data	with sign-bit amplitude data
depth in feet of the reflector	2000.	2000.
jump in feet/sec. at X=1000ft, Z=2000ft	495.252	368.513
error in amplitude (%)	-0.95	-26.3

Table IV.A2

the amplitude of the jump is smaller.

A2.-N/S=0.5

Another example is set with N/S=0.5. The processed time sections with true amplitude data and with sign-bit data are represented on Figure IV.A2.1 and on Figure IV.A2.3 respectively. Then the velocity computation is performed with each of these processed time sections; the outputs of these computations are shown on the Figure IV.A2.2 and on Figure IV.A2.4 respectively. The reflector is delimited at the right depth on each of the plots. The numerical results are displayed in the table IV.A2.

A3.-N/S=1.0

Another example is set with N/S=1.0. The processed time sections with true amplitude data and with sign-bit data are represented on Figure IV.A3.1 and on Figure IV.A3.3 respectively. Then the velocity computation is performed with each of these processed time sections; the outputs of these computations are shown on the Figure IV.A3.2 and on Figure IV.A3.4 respectively. The reflector is delimited at the right depth on each of the plots. The numerical results are displayed in the table IV.A3.

A4.-N/S=25.6

Now a bigger noise is created with N/S=25.6. The synthetic time

OUTPUT OF THE VELOCITY COMPUTATION
WITH ONE HORIZONTAL REFLECTOR, N/S=0.2

	with true amplitude data	with sign-bit amplitude data
depth in feet of the reflector	2000.	2000.
jump in feet/sec. at X=1000ft,Z=2000ft	491.697	384.367
error in amplitude (%)	-1.66	-23.126

Table IV.A1

IV. Effects of the noise on the computation.

A. Using one bit to replace the amplitude.

The effects of the noise will be studied in the example of one horizontal plane located at 2000ft under the ground (see data in Appendix B). When the noise-to-signal ratio (N/S) is not equal to zero, a wave field is created by the subroutine NOISE and is added to the scattered wave field at each sample point. The resulting wave field is processed in the same way as in the previous examples. Sign-bit processing will be completed with +1 and -1 as before.

A1.-N/S=0.2

A first example is set with N/S=0.2. The processed time sections with true amplitude data and with sign-bit data are represented on Figure IV.A1.1 and on Figure IV.A1.3 respectively. Then the velocity computation is performed with each of these processed time sections; the outputs of these computations are shown on the Figure IV.A1.2 and on Figure IV.A1.4 respectively. The reflector is delimited at the right depth on each of the plots. The numerical results are displayed in the table IV.A1.

The noise did not affect the good location of the reflector but

OUTPUT OF THE VELOCITY COMPUTATION
WITH AN ARC OF CIRCLE, NO NOISE

	with true amplitude data	with sign-bit amplitude data
depth in feet at X=1000 Z=1000	1000.	1000.
jump in feet/sec. at (1000,1000)	454.	418.
error in amplitude in %	-9.2	-16.4

Table III.E

V. CONCLUSION.

Based on the configuration examples, the following conclusions have been drawn concerning sign-bit processing on a linear backscatter array:

(1) In the examples tested, the output of the velocity inversion algorithm with sign-bit amplitude processing is within 10% to 20% of the one with true amplitude data processing.

(2) Moreover the jumps in velocity computed in both cases are of the same order as the jump given in the data for GE02D, as long as the noise-to-signal ratio is not too large.

(3) In both processings the noise does not prevent the good location of the reflecting subsurface, as long as the noise-to-signal ratio is reasonable.

(4) For small noise-to-signal ratios, the error from sign-bit data processing is larger than the error from true amplitude data processing. Thus the noise burst problems with the Born inversion algorithm are not always minimized by only using the sign-bit, which is in contrast with the remark stated by Martin et al. (1975).

VI. REFERENCES

1. Alihilali, K. A., and Musick, A., 1975,
An evaluation of sign-bit seismic recording and its impact on processing and interpretation: Geophysics, vol. 40, p. 129.

2. Bleistein, N., Cohen, J.K., and Hagin, F.G., 1984,
Computational and asymptotic aspects of velocity inversion.

3. Bleistein, N., Cohen, J.K., 1982,
The velocity inversion problem. Present status, new directions.

4. Bleistein, N., 1984,
Two-and-one-half dimensional in-plane wave propagation.

5. Fort, J. R., Wetsphal, J. A., Dix, C. H., Martin, L. A., and Allen, S. J., 1973,
A new multichannel data acquisition and processing system: Geophysics, vol. 38, p. 1198.

6. Gimlin, D. R., and Smith, J. W., 1980,
A comparison of seismic trace summing techniques: Geophysics, vol. 45, p. 1017-1041.

7. Hagin, F. G., and Cohen, J. K., 1984.
Refinements to the linear velocity inversion theory: Geophysics, vol. 49, no. 2, p. 112-118.

8. Martin, L. A., Allen, S. J., and Jeffer, R. H. F., 1975,
Noise burst problems with Vibroseis minimized by using only the sign-bit: Geophysics, vol. 40. p. 139.

9. O'Brien, J. T., Kamp, W. P., and Hoover, G. M., 1982
Sign-bit amplitude recovery with application to seismic data: Geophysics, vol. 47, no. 11, p. 1526-1539.

10. Schoellohorn, S. W., and Neal, G., 1975,
Sign-bit summing: Geophysics, vol. 42, p. 1540.

11. Shirley, T. E., Linville, A. F., and Spratt, R. S., 1983,
Analysis of sign-bit recording for high and low noise environments: 53th SEG extended abstract.

12. Yuan-Cheng Lee, 1984,
Analysis of sign-bit recording for synthetic vibrator data: PHD thesis in Colorado School of Mines.

VII. FIGURES

SYNTHETIC TIME SECTION

FROM 1 HORIZONTAL REFLECTOR, N/S=0.0

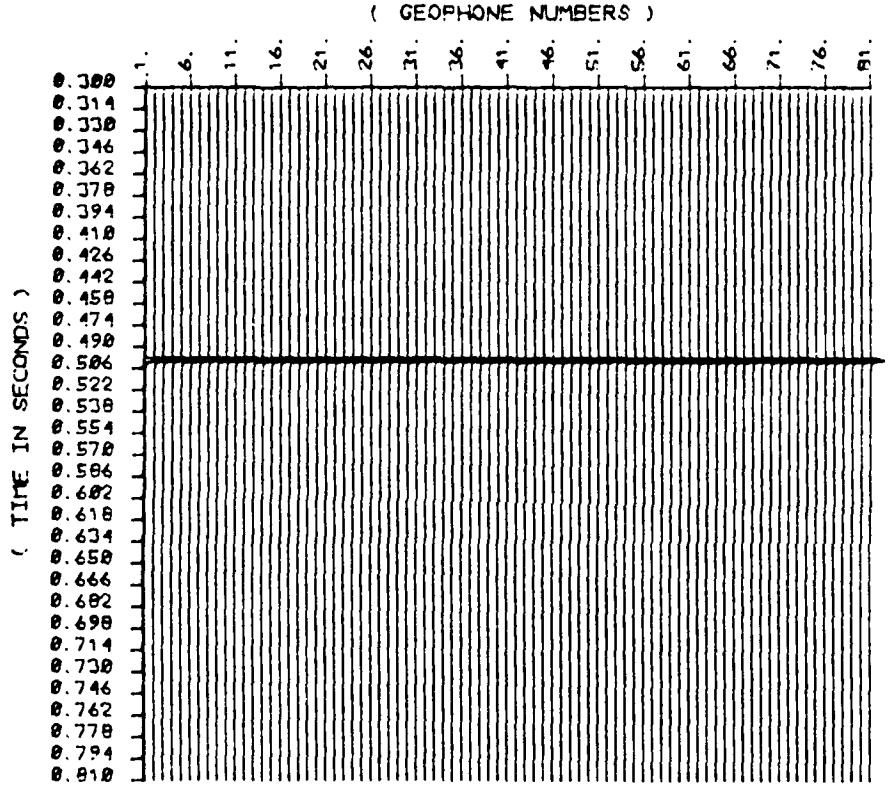

FIGURE III.A.1

PROCESSED TIME SECTION
WITH TRUE DATA
FROM 1 HORIZONTAL REFLECTOR. N/S=0.0

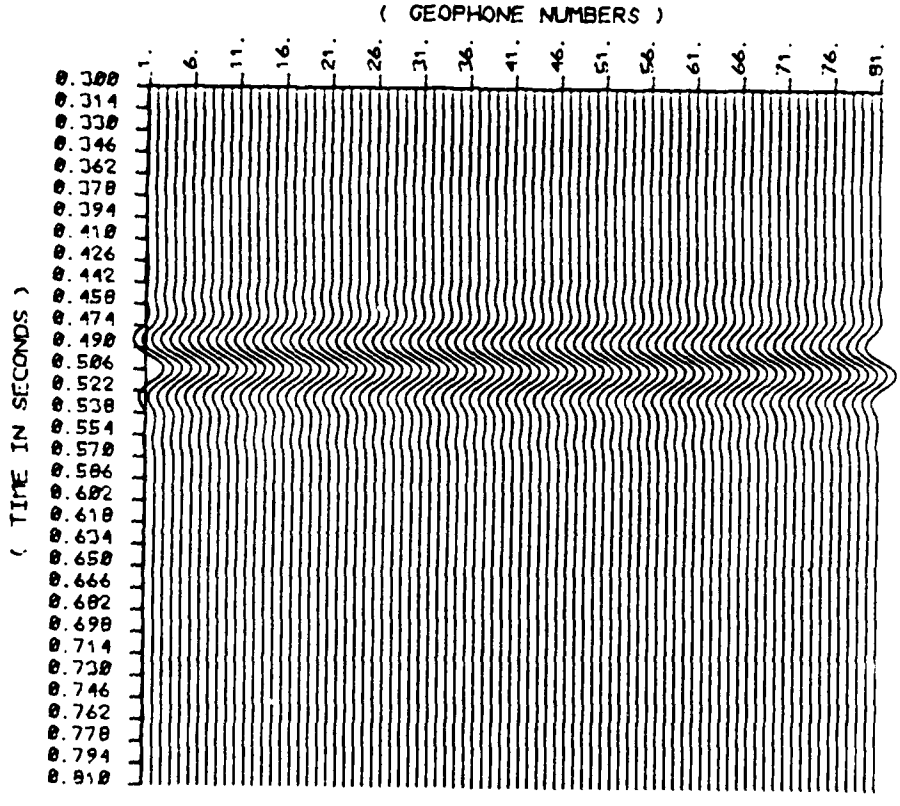

FIGURE III.A.2

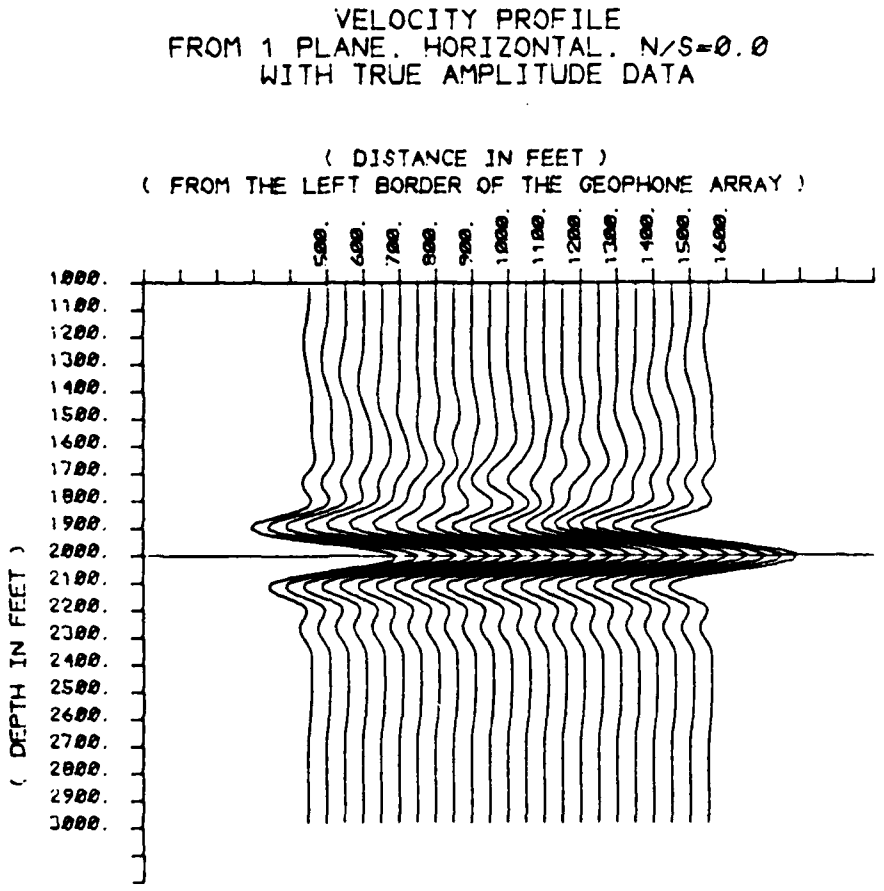

FIGURE III.A.3

PROCESSED TIME SECTION
WITH SIGN-BIT AMPLITUDE DATA
FROM 1 PLANE. HORIZONTAL. N/S=0.0.

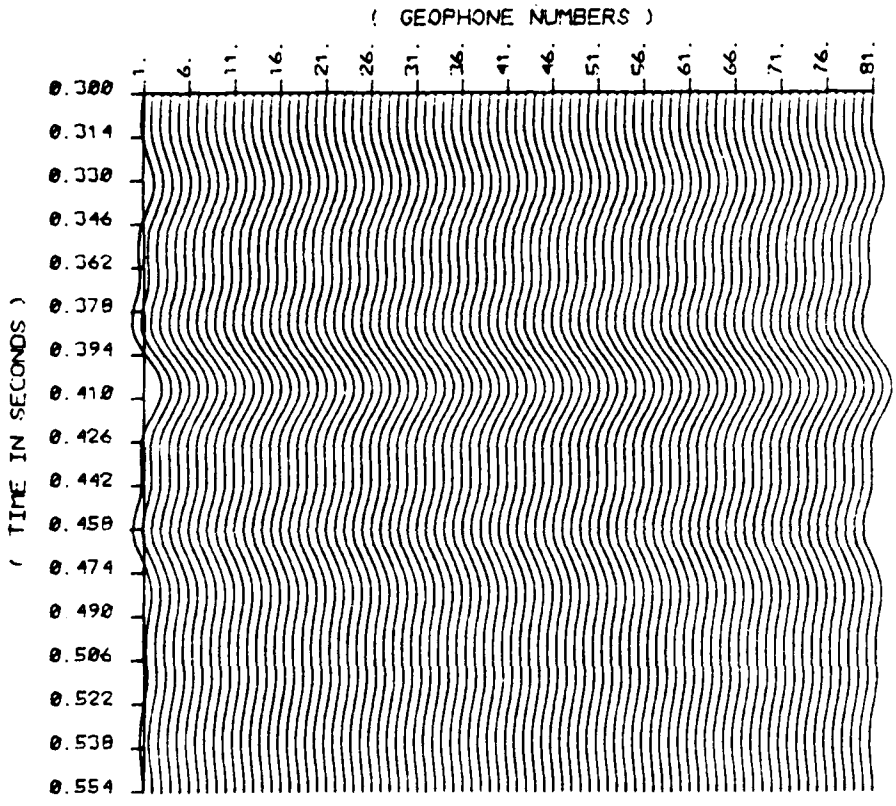

FIGURE III.A.4

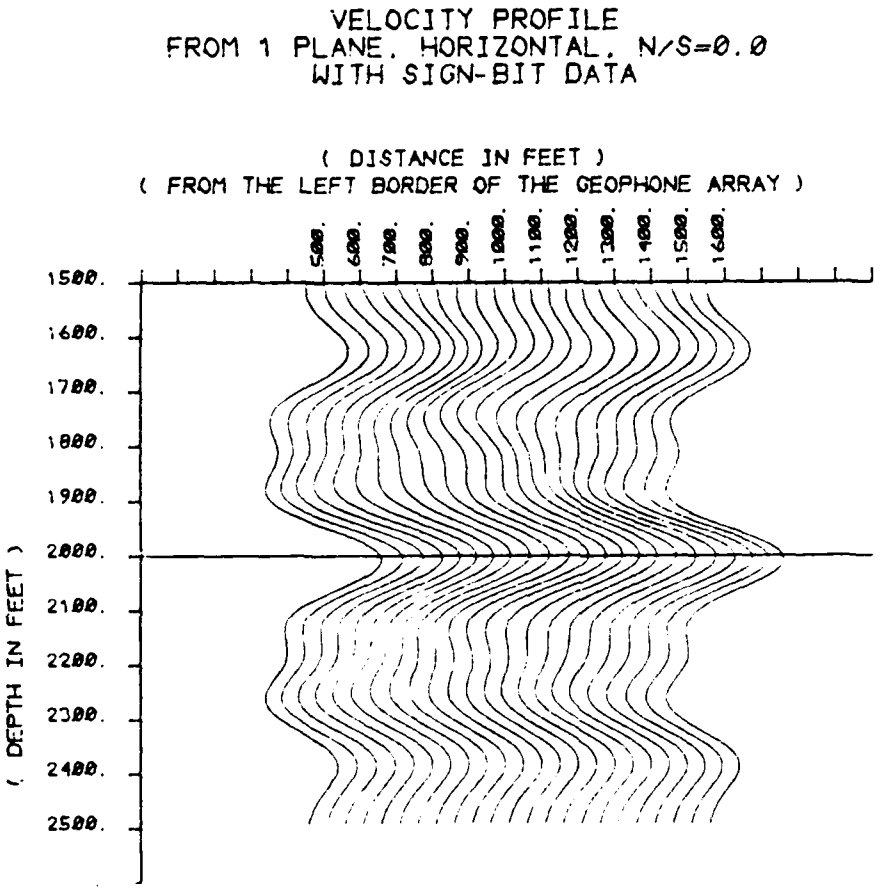

FIGURE III.A.5

SYNTHETIC TIME SECTION

FROM 1 TILTED REFLECTOR. N/S=0.0

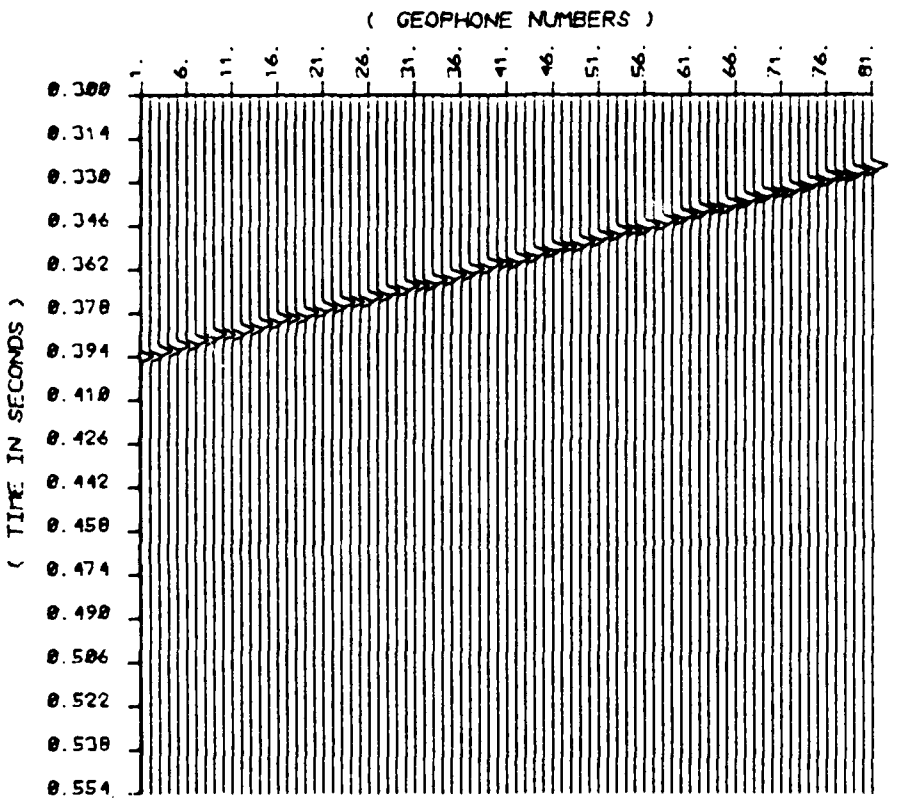

FIGURE III.B.1

PROCESSED TIME SECTION
WITH TRUE AMPLITUDE DATA
FROM 1 PLANE, TILTED 10 DEG. N/S=0..

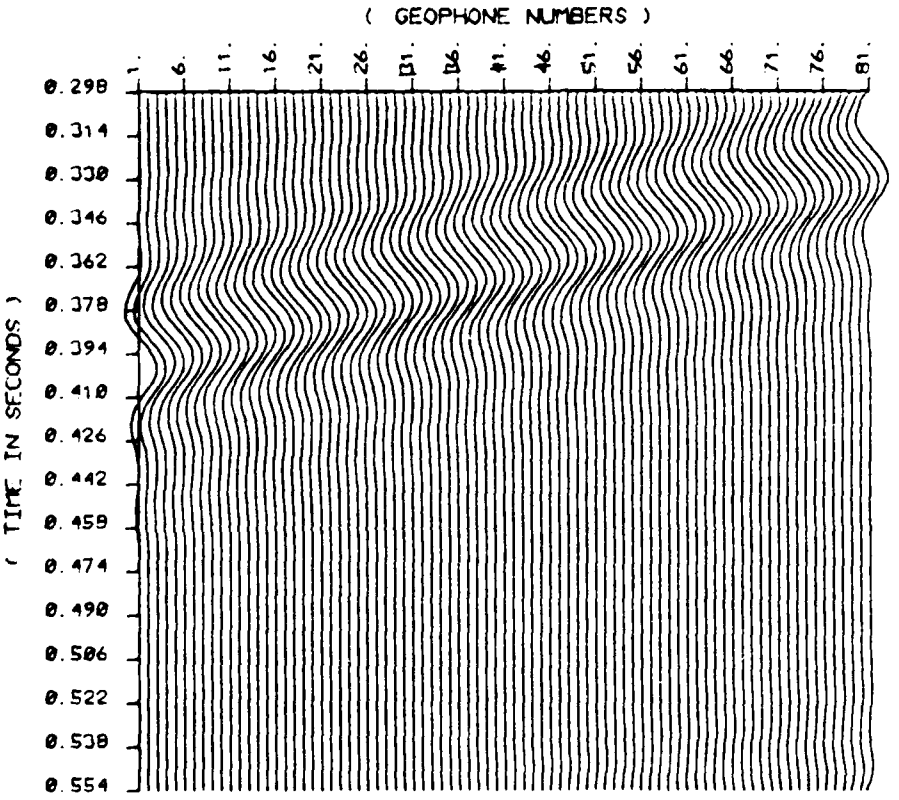

FIGURE III.B.2

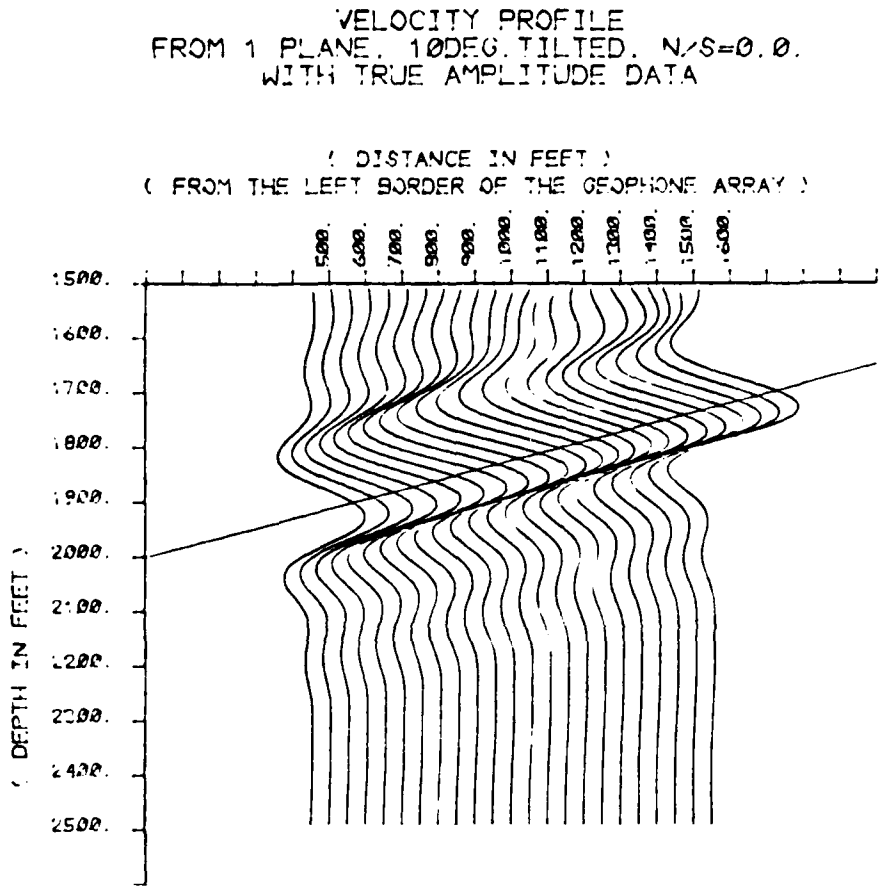

FIGURE III.B.3

PROCESSED TIME SECTION
WITH SIGN-BIT AMPLITUDE DATA
FROM 1 PLANE. 10 DEG TILTED. N/S=0.0.

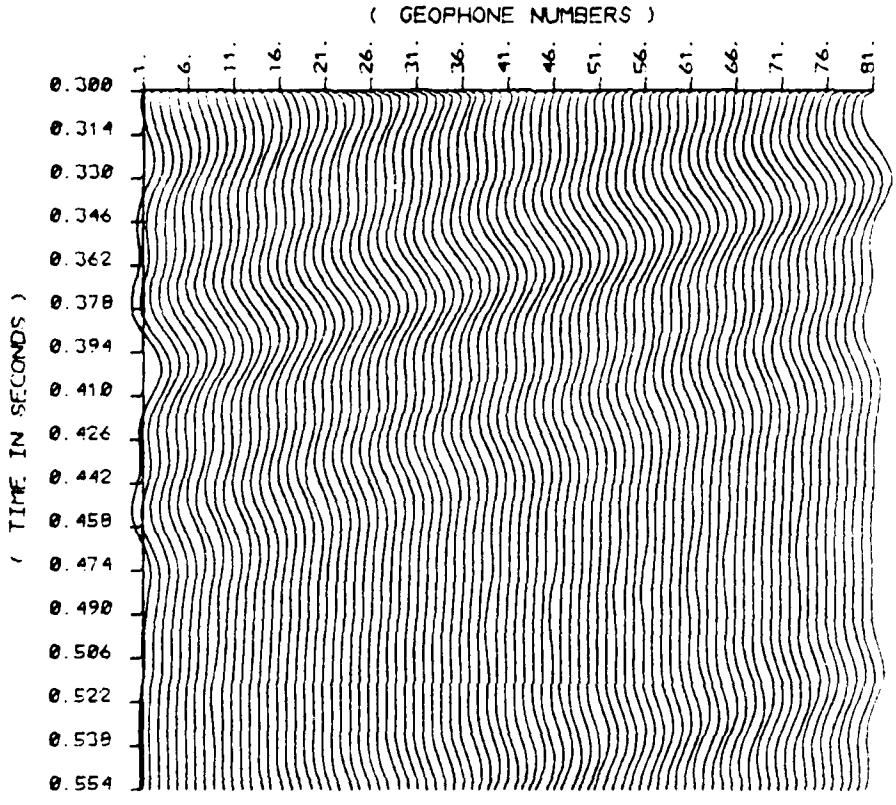

FIGURE III.B.4

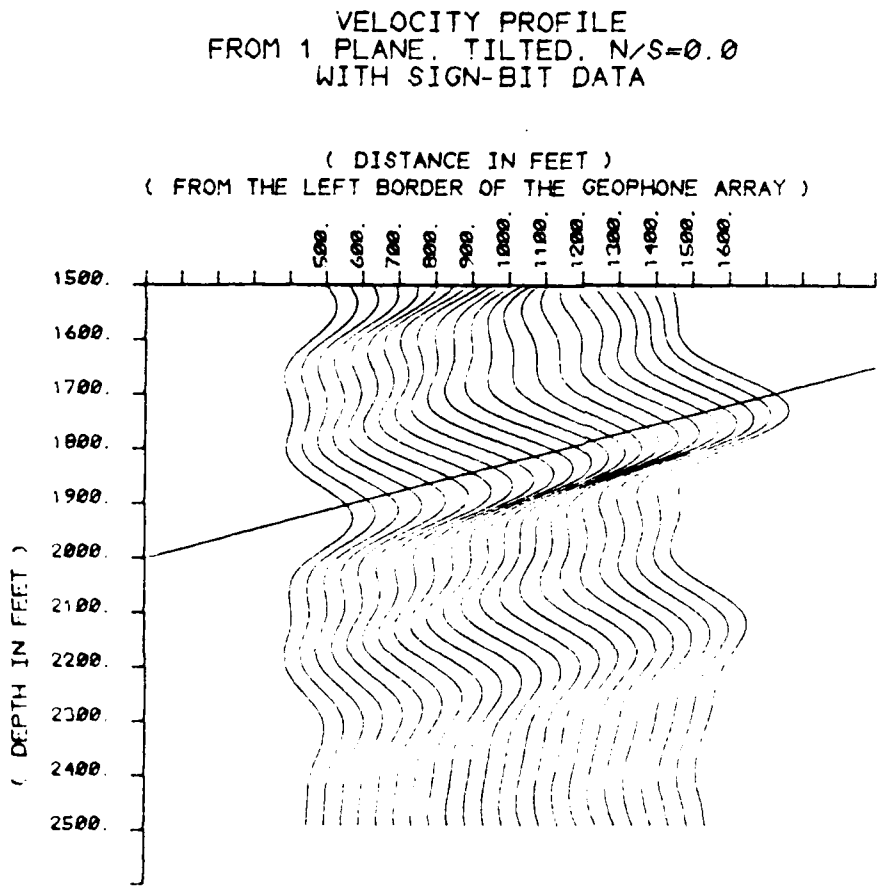

FIGURE III.B.5

SYNTHETIC TIME SECTION

FROM 2 HORIZONTAL REFLECTORS. N/S=0.0

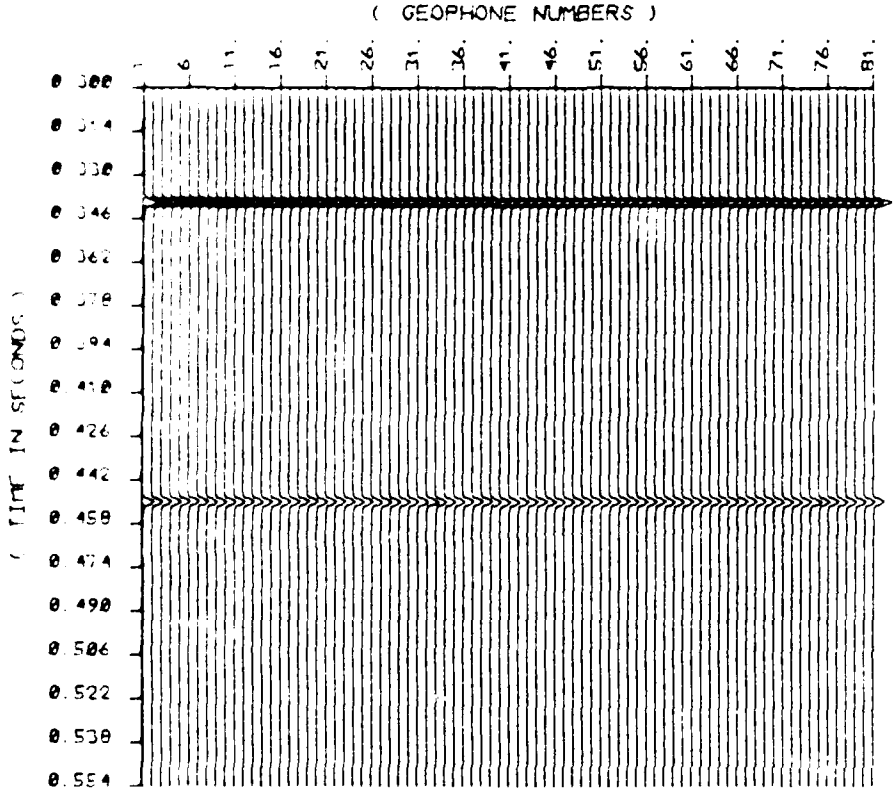

FIGURE III.C.1

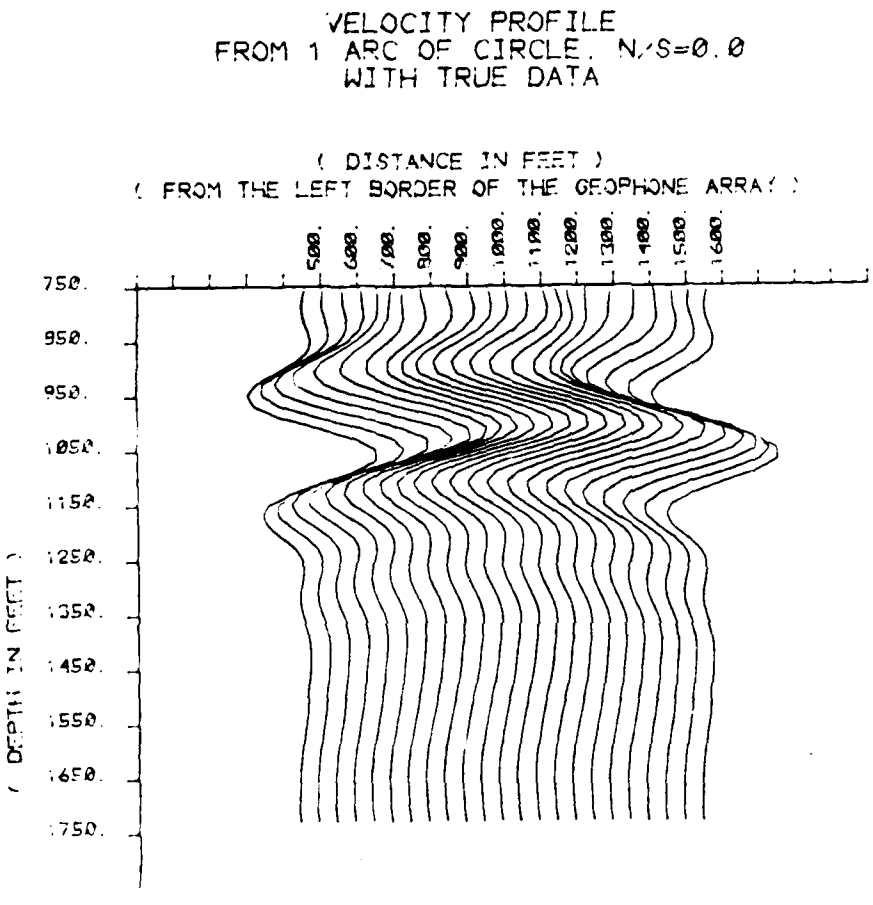

FIGURE III.B.3

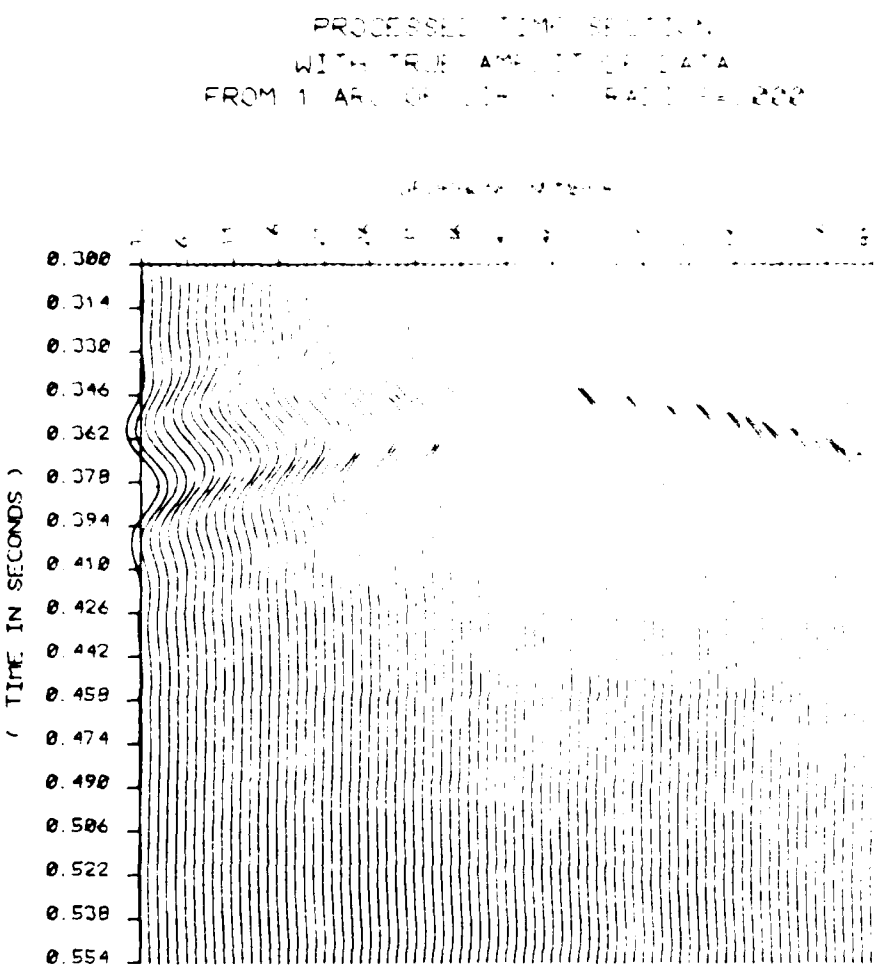

FIGURE III.E.2

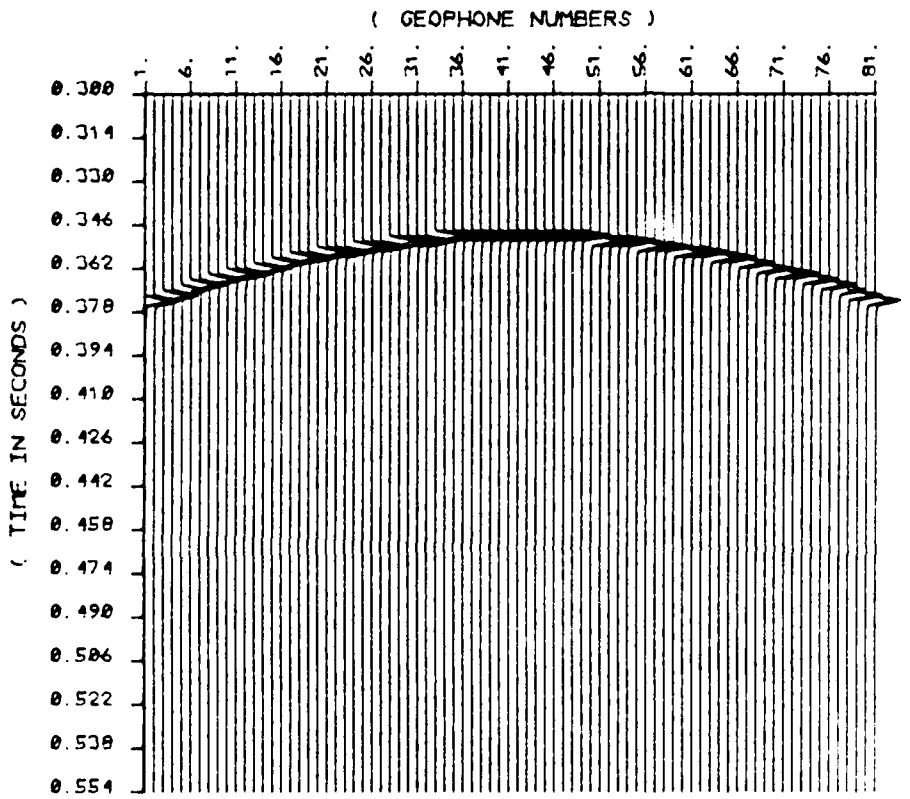

FIGURE III.E.1

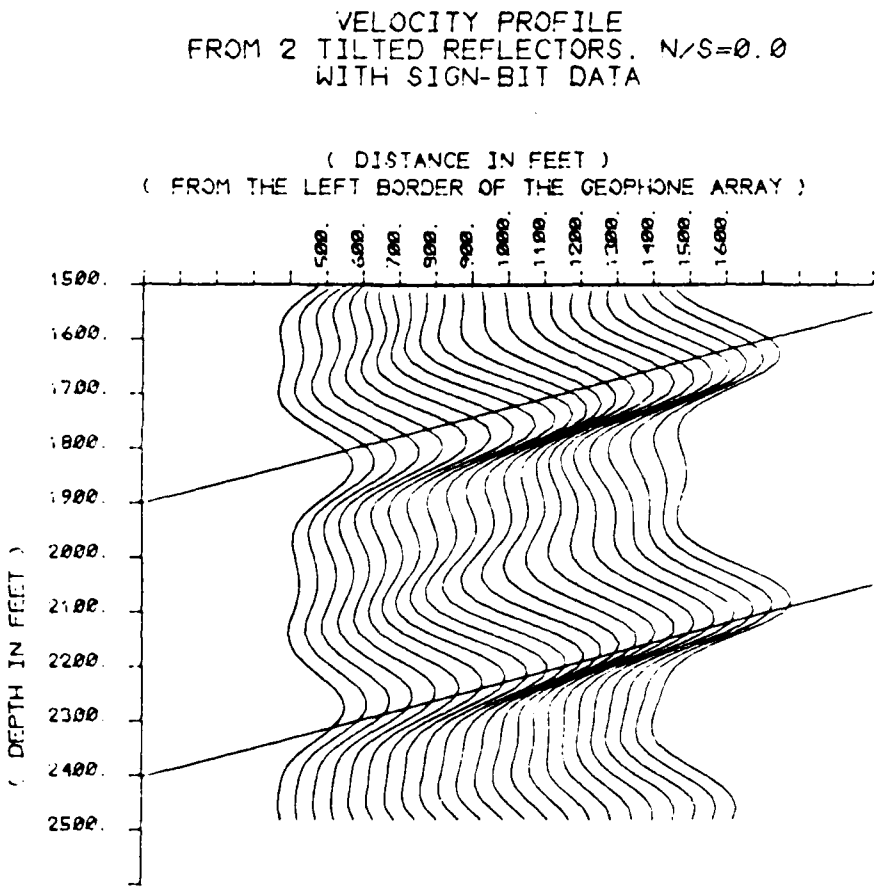

FIGURE III.D.5

PROCESSED TIME SECTION
WITH SIGN-BIT DATA
FROM 2 TILTED REFLECTORS. N/S=0.0.

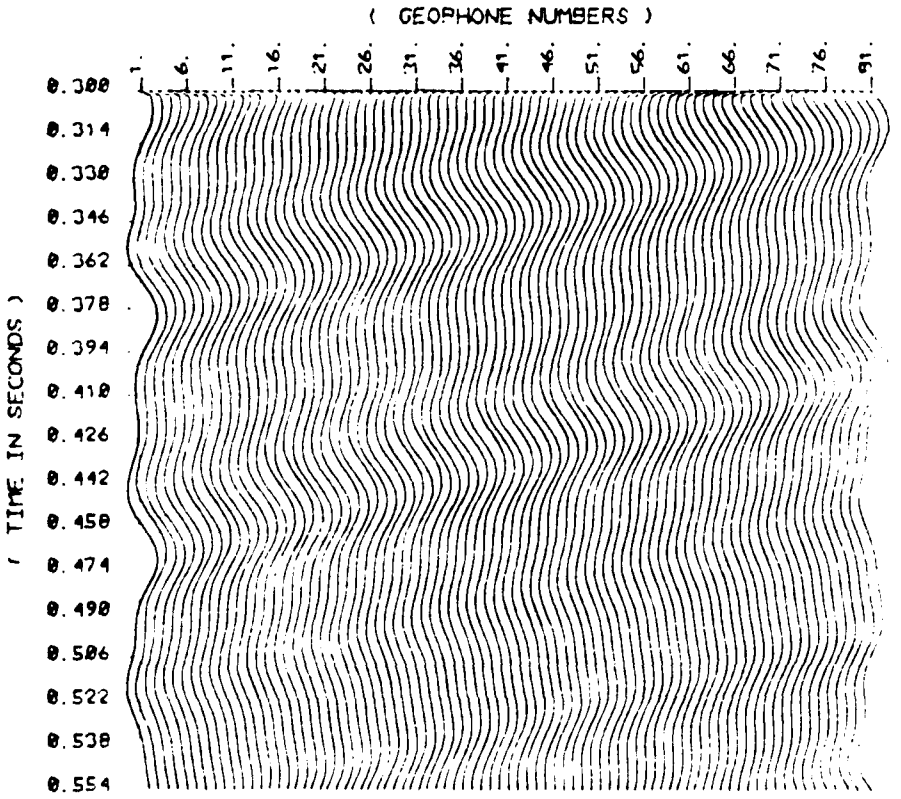

FIGURE III.D.4

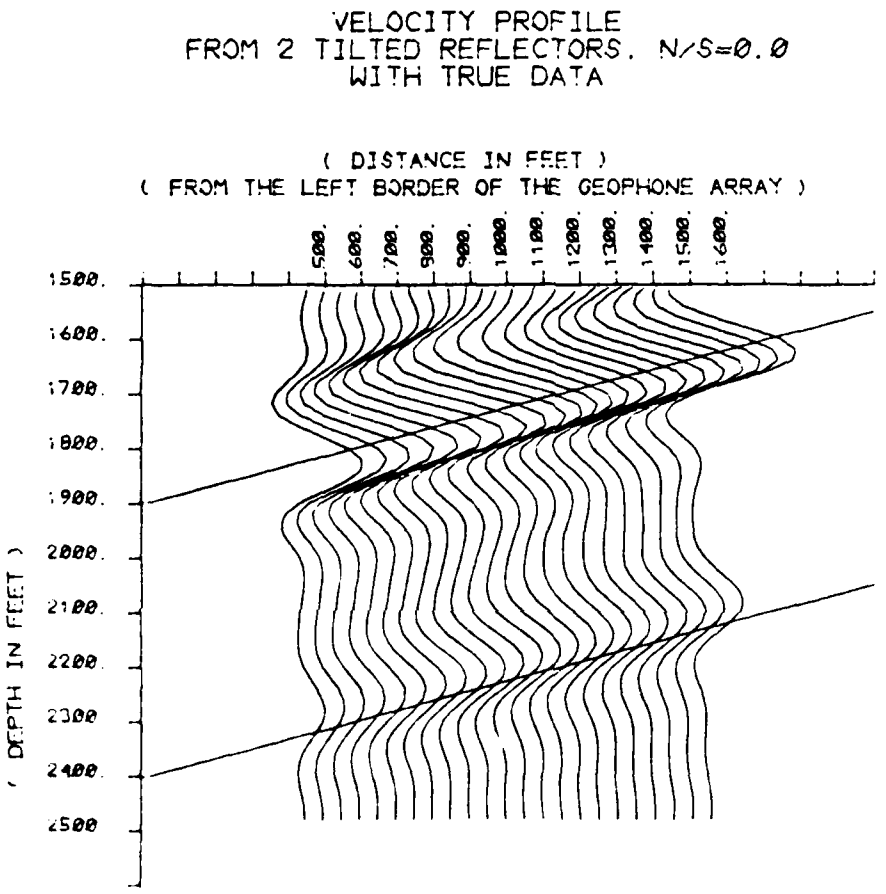

FIGURE III.D.3

PROCESSED TIME SECTION
WITH TRUE DATA
FROM 2 TILTED REFLECTORS. N/S=0.0

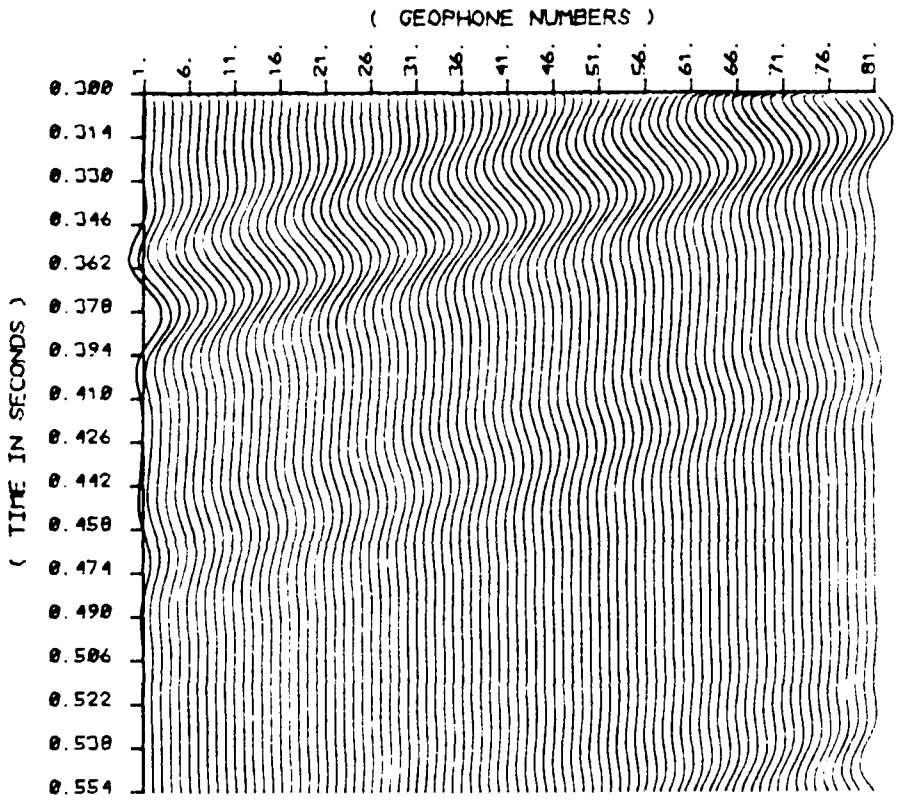

FIGURE III.D.2

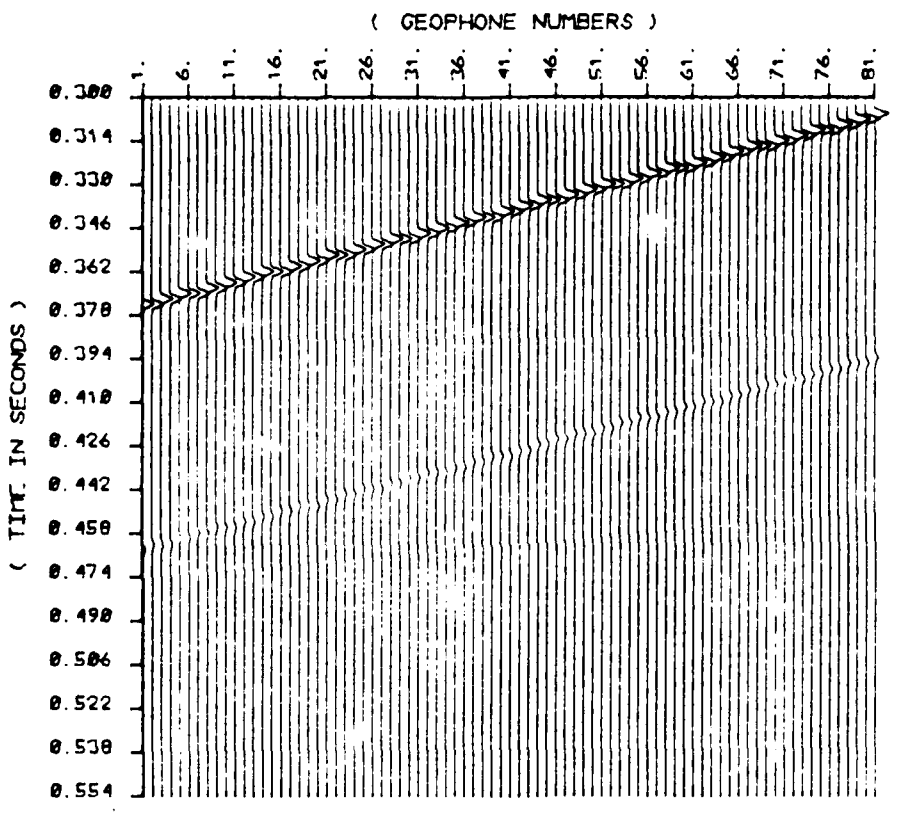

FIGURE III.D.1

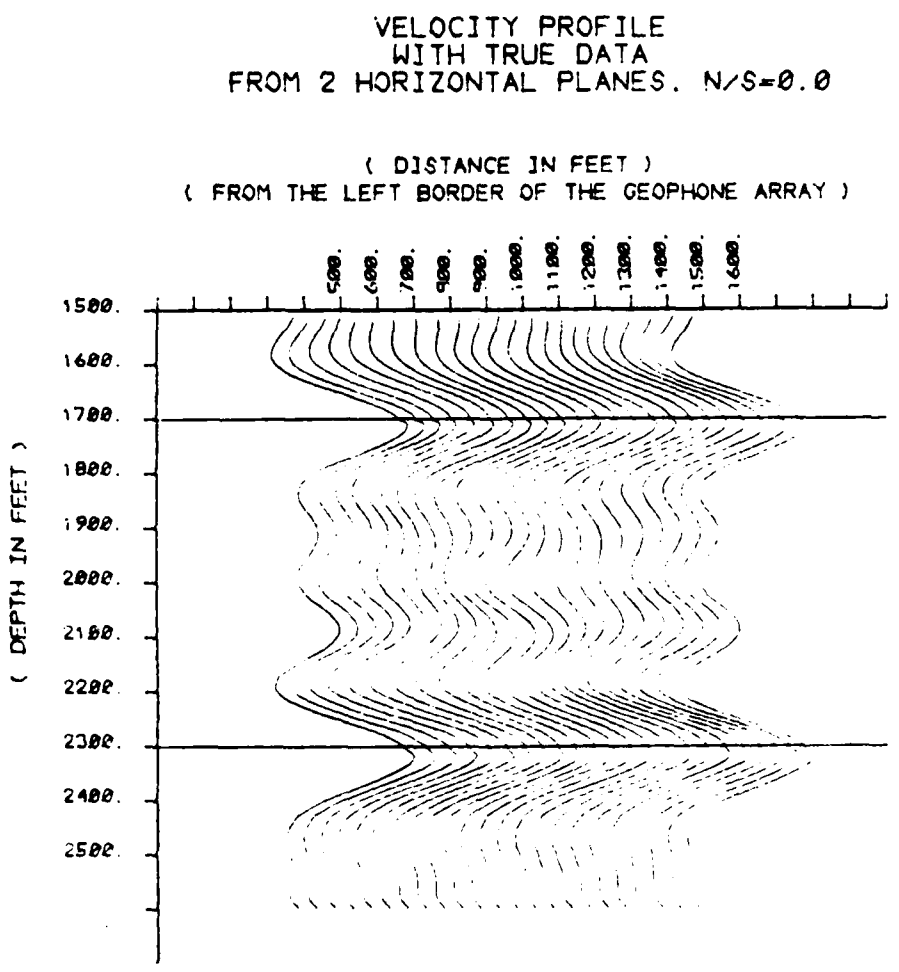

FIGURE III.C.7

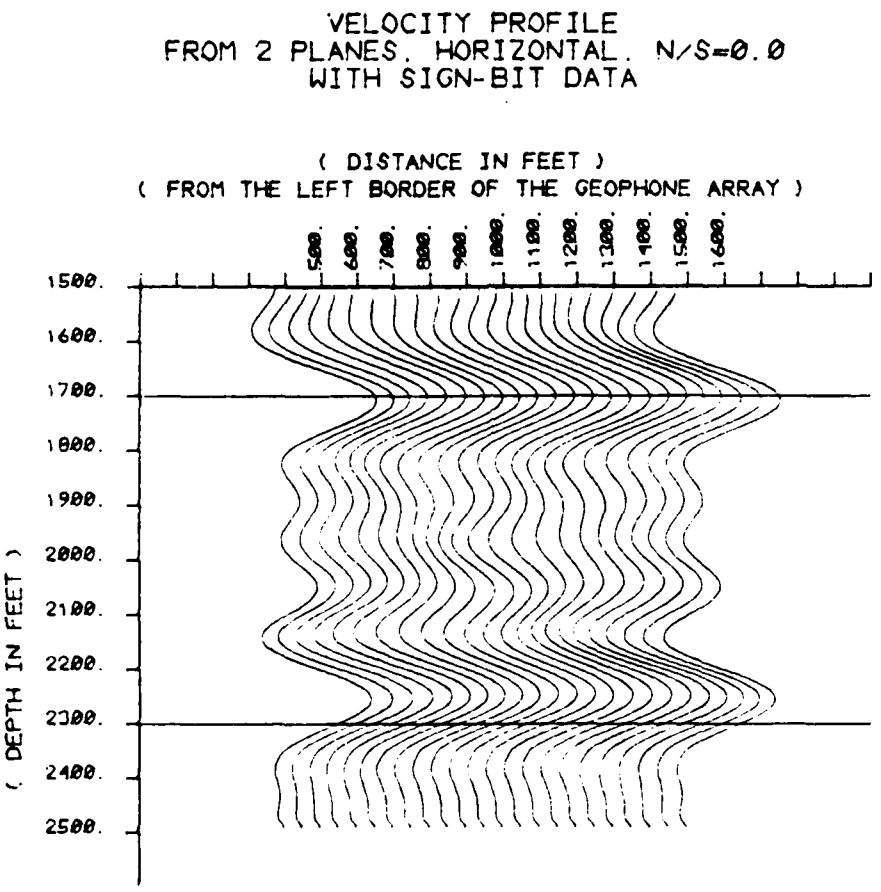

FIGURE III.C.6

PROCESSED TIME SECTION
WITH SIGN-BIT AMPLITUDE DATA
FROM 2 PLANES. HORIZONTAL. N/S=0.0.

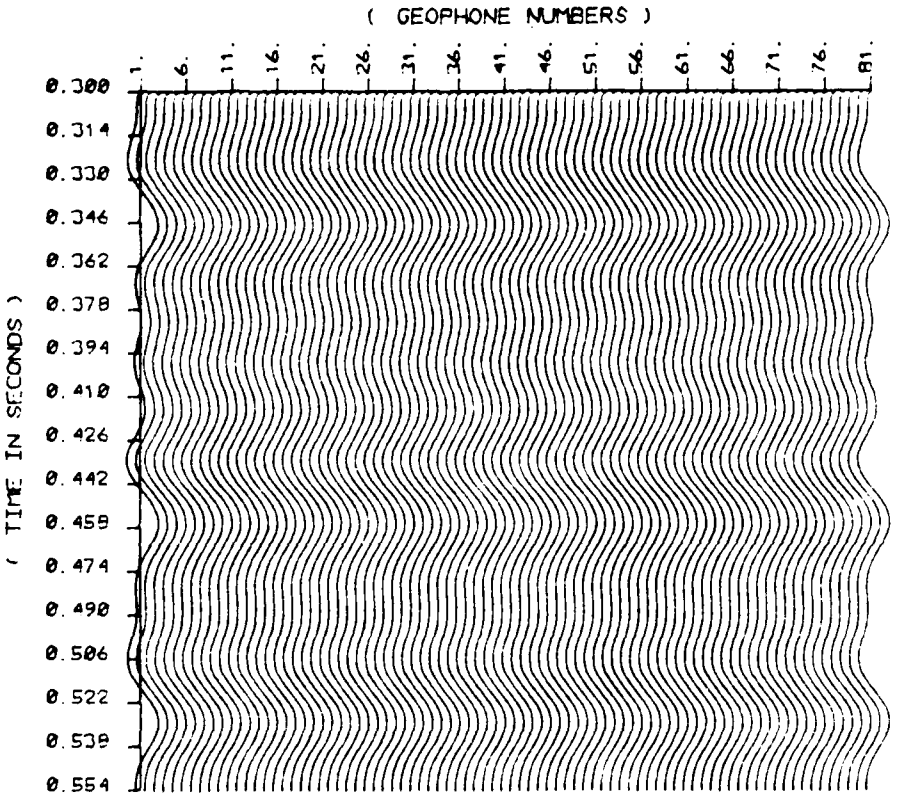

FIGURE III.C.5

VELOCITY PROFILE
WITH TRUE DATA
FROM 2 HORIZONTAL PLANES. N/S=0.0

(DISTANCE IN FEET)
(FROM THE LEFT BORDER OF THE GEOPHONE ARRAY)

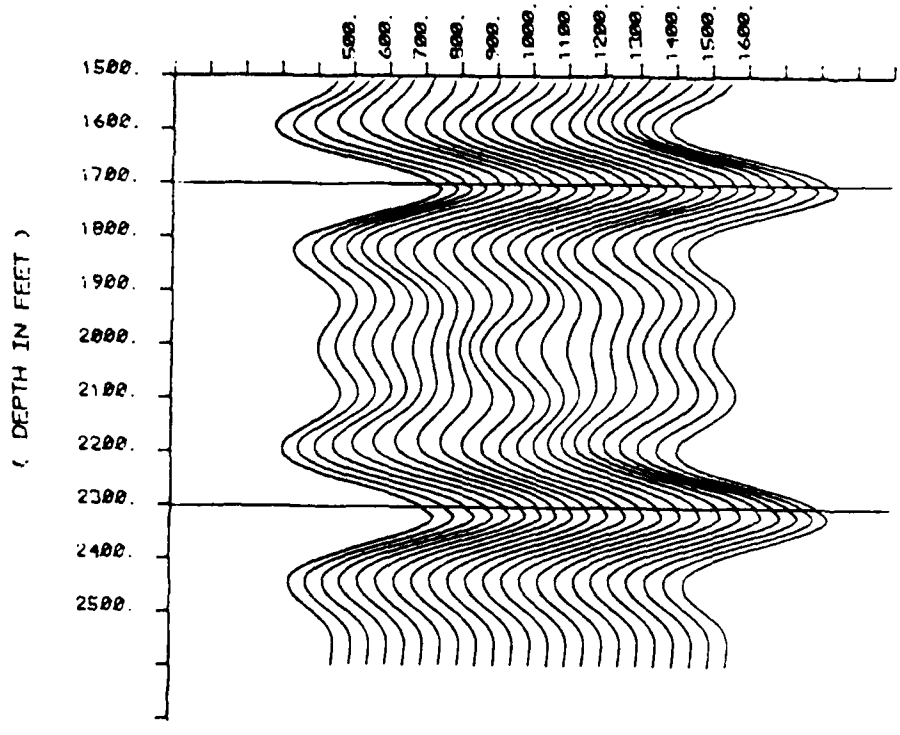

FIGURE III.C.4

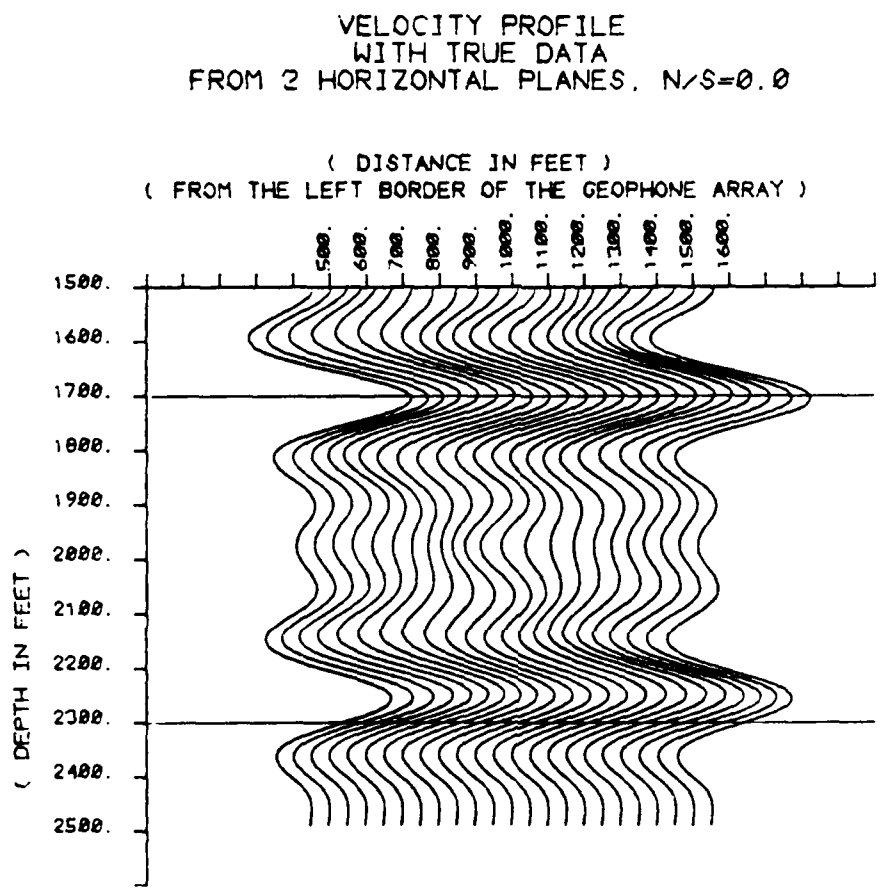

FIGURE III.C.3

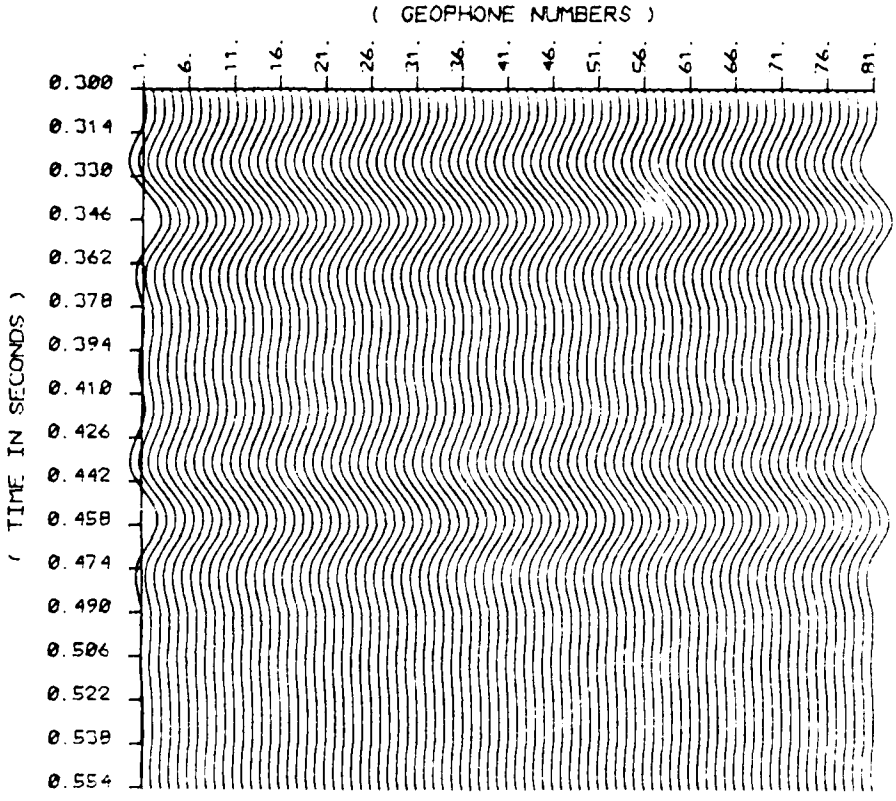

FIGURE III.C.2

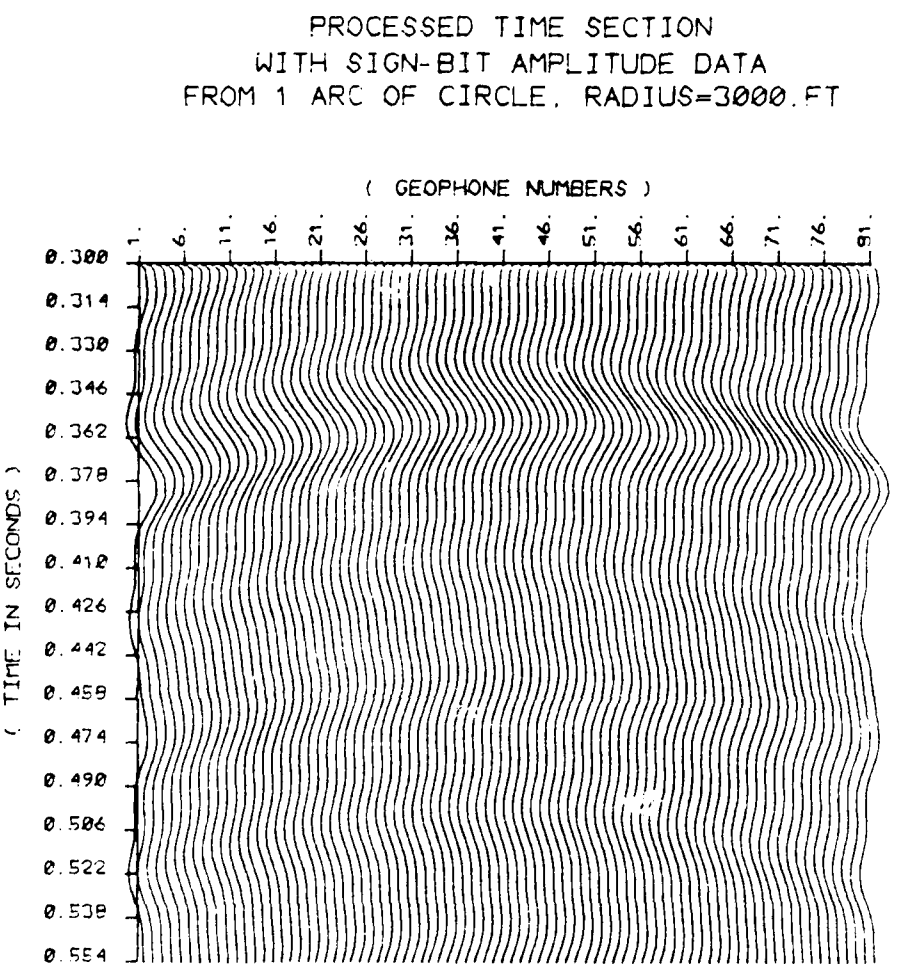

FIGURE III.E.4

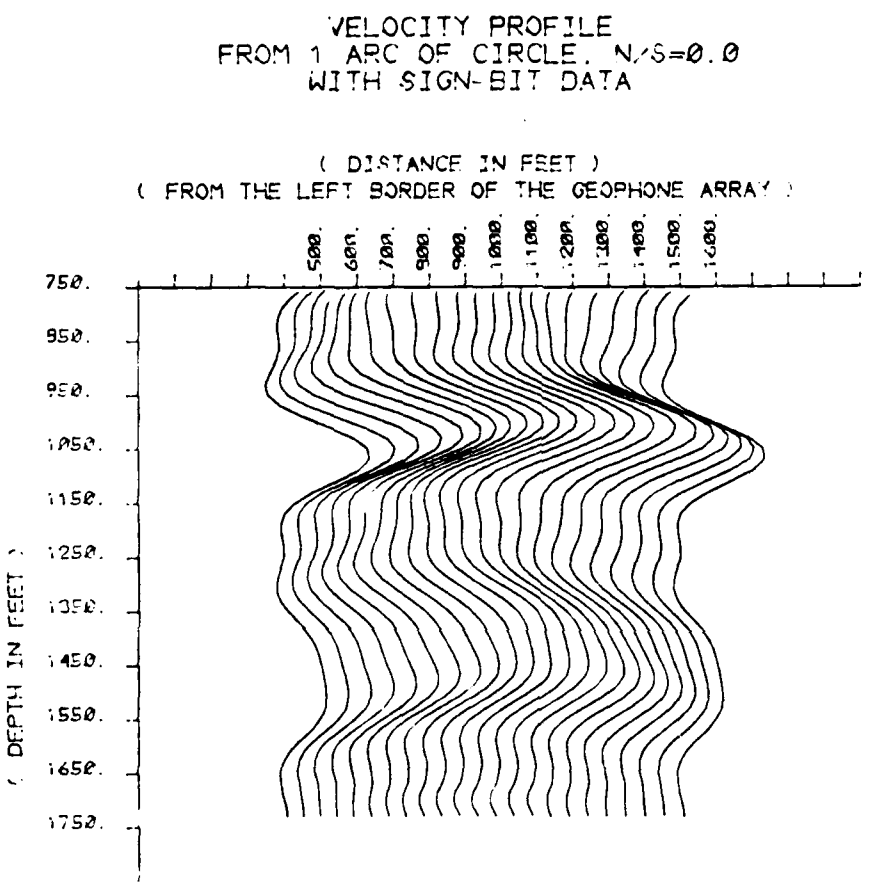

FIGURE III.B.5

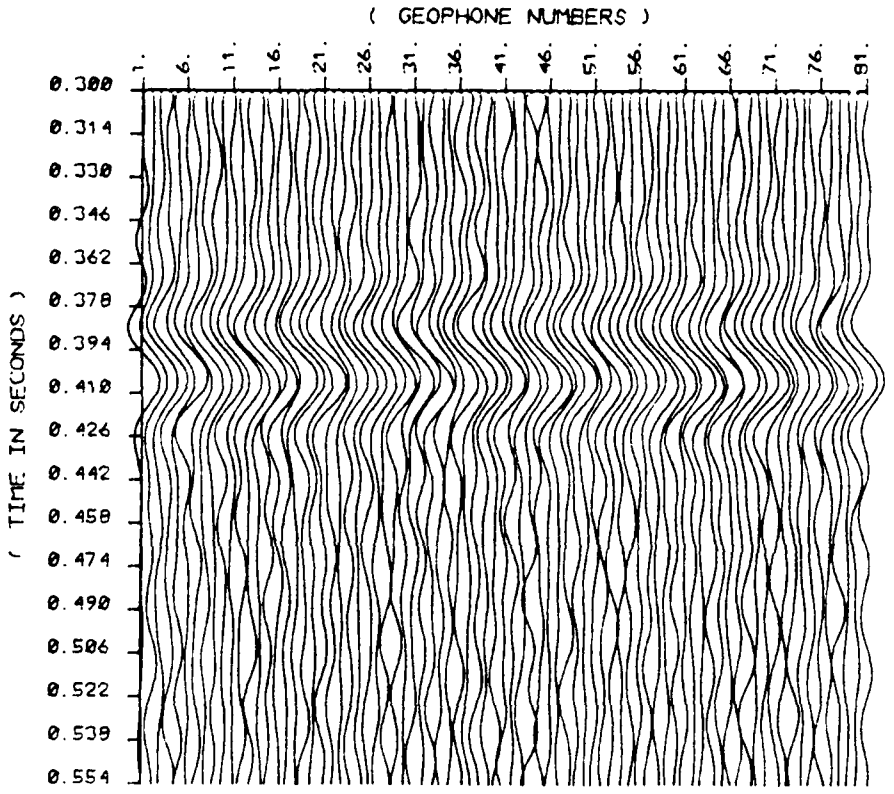

FIGURE IV.A1.1

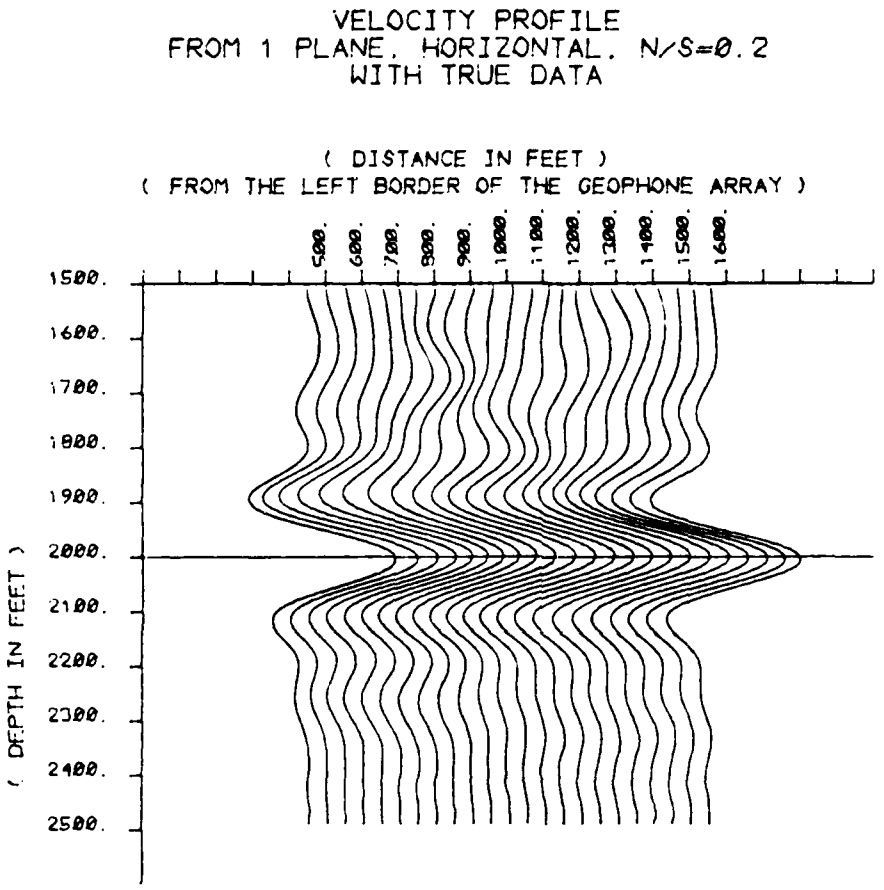

FIGURE IV.A1.2

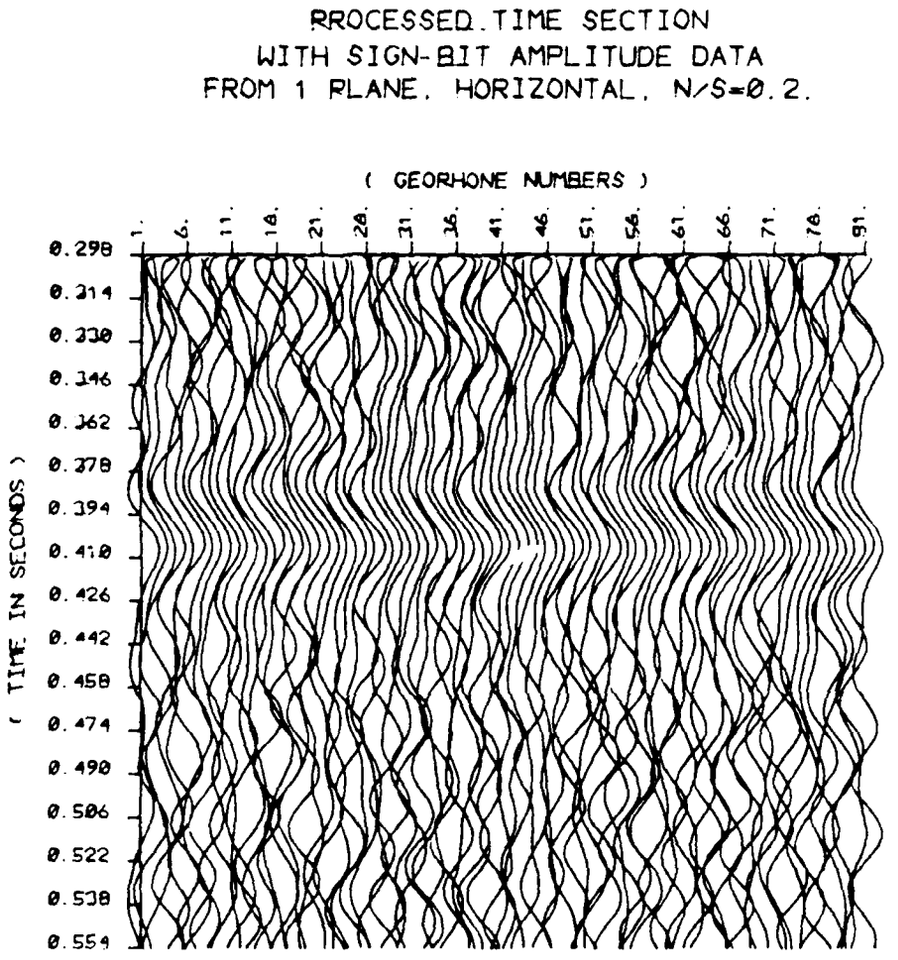

FIGURE IV.A1.3

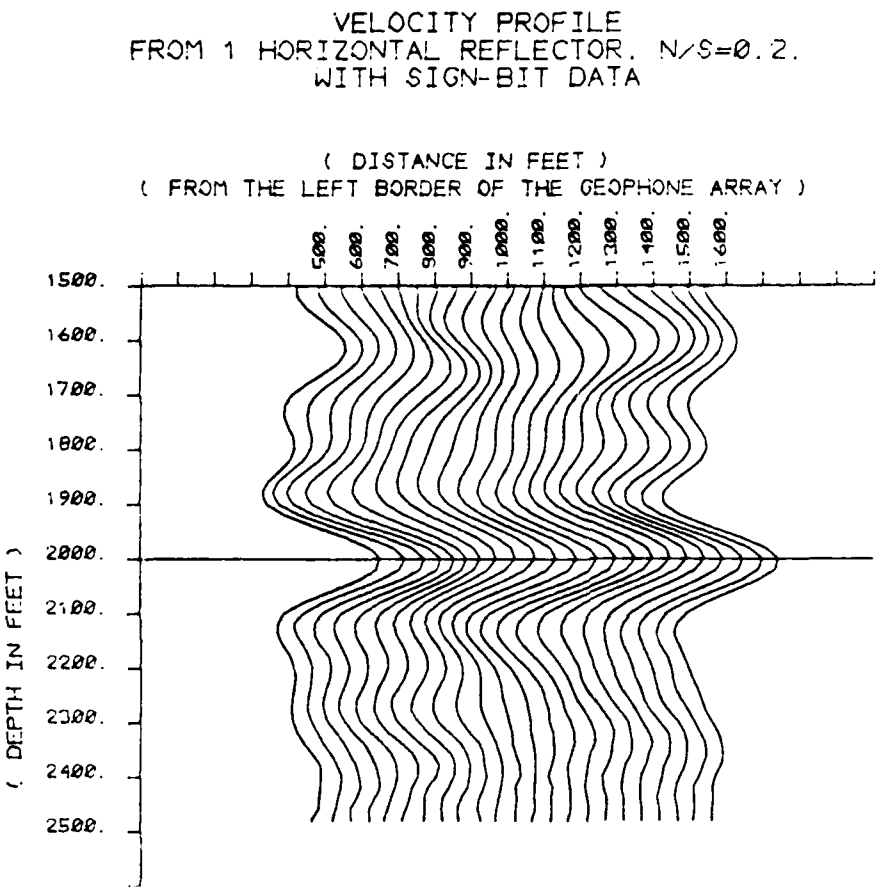

FIGURE IV.A1.4

SYNTHETIC TIME SECTION

FROM 1 HORIZONTAL REFLECTOR. N/S=0.5

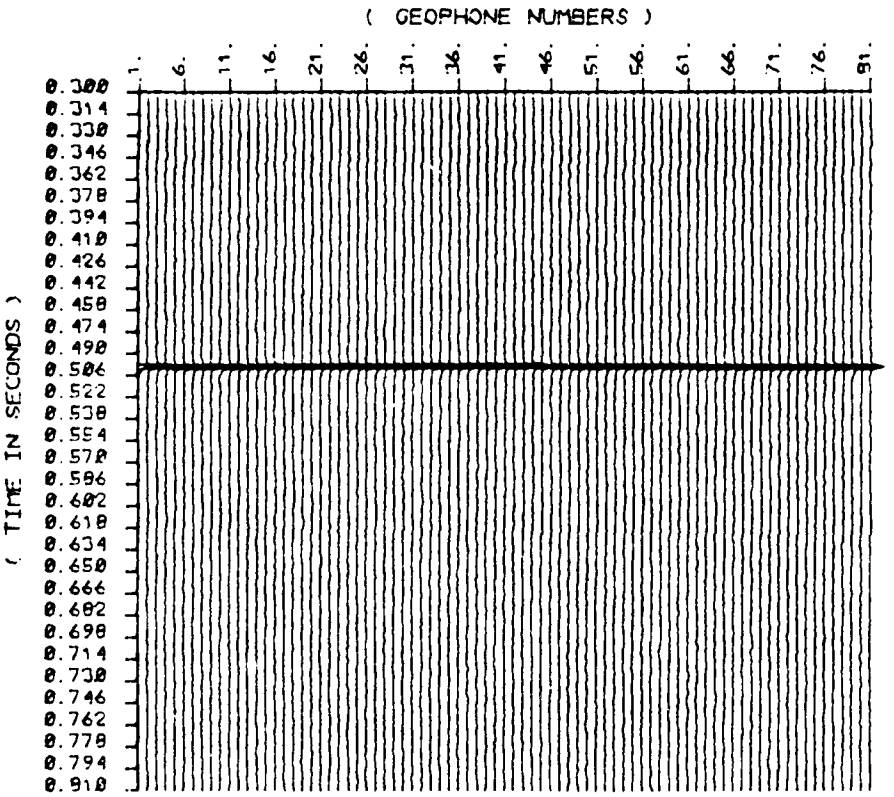

FIGURE IV.A2.1

PROCESSED TIME SECTION
WITH TRUE DATA
FROM 1 HORIZONTAL REFLECTOR. N/S=0.5.

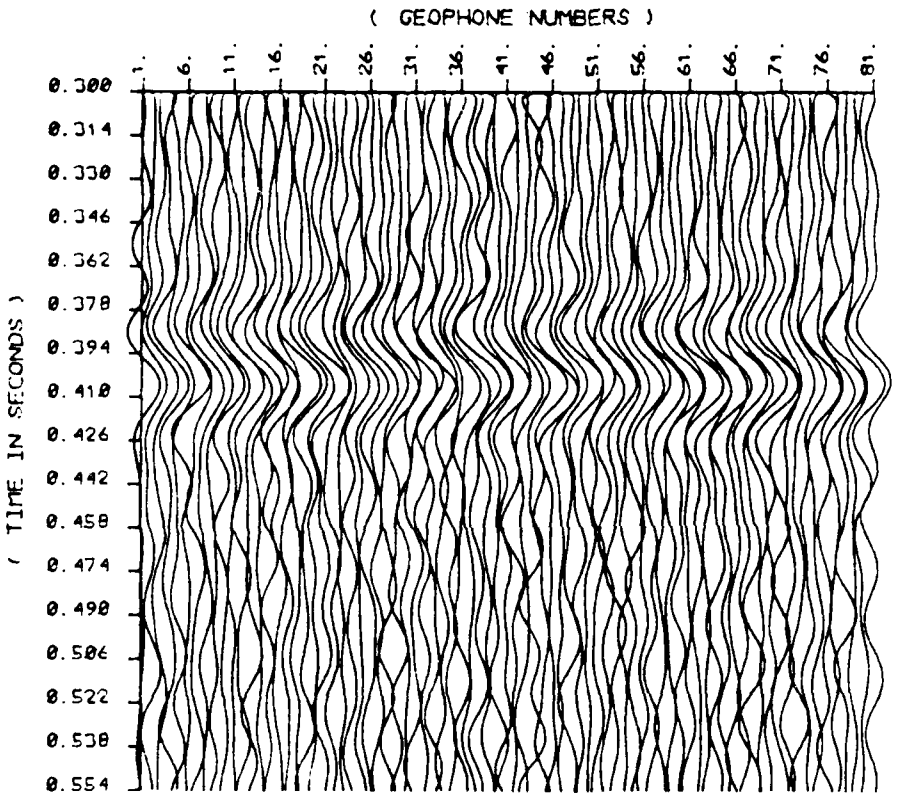

FIGURE IV.A2.2

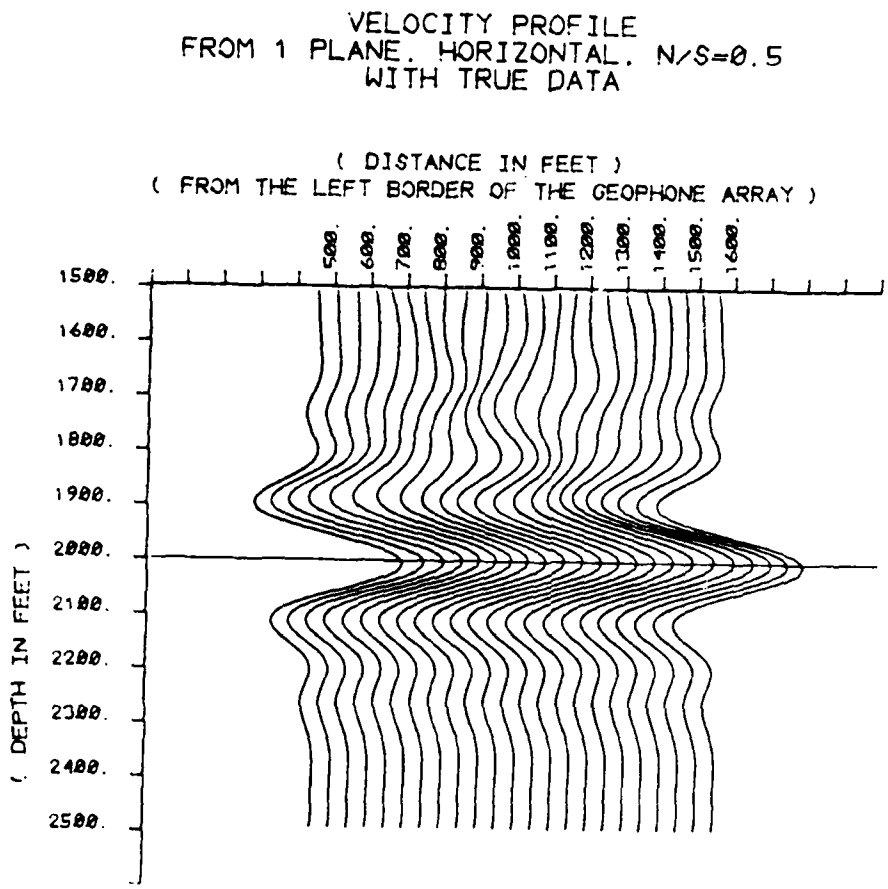

FIGURE IV.A2.3

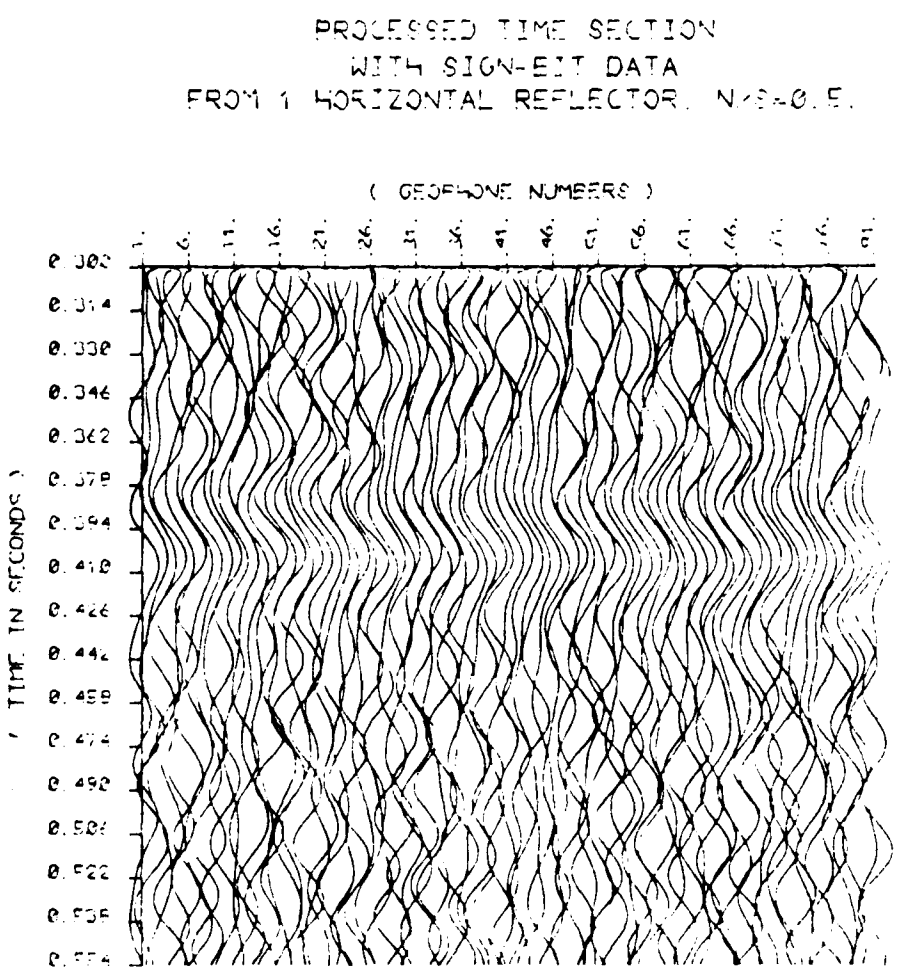

FIGURE IV.A2.4

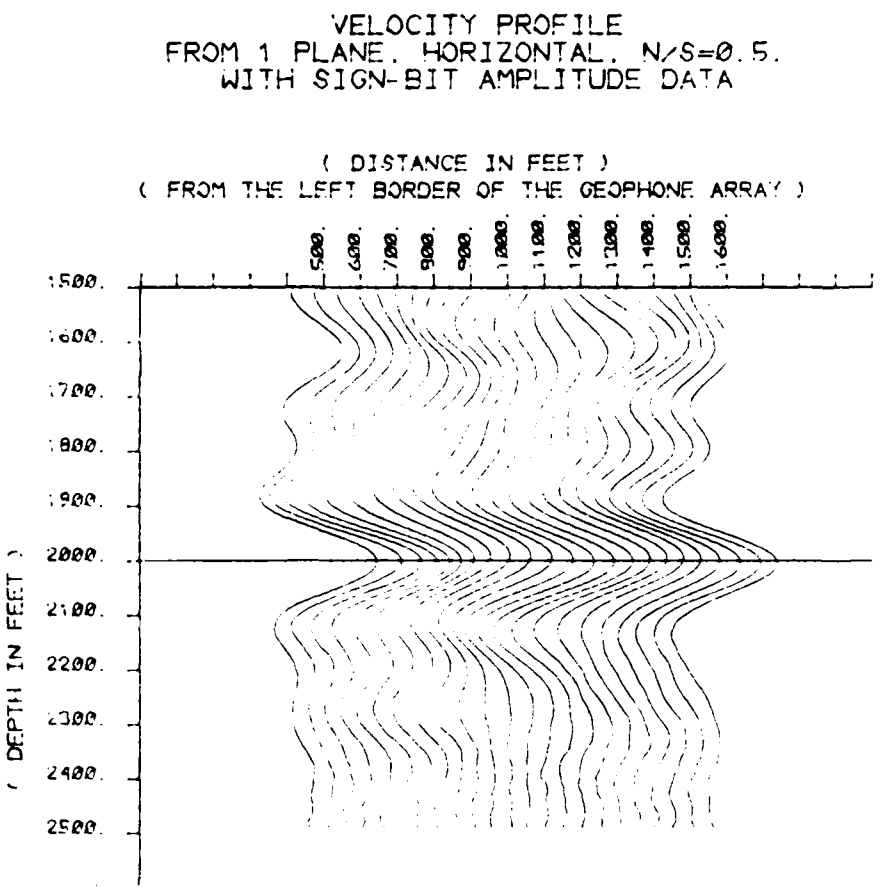

FIGURE IV.A2.5

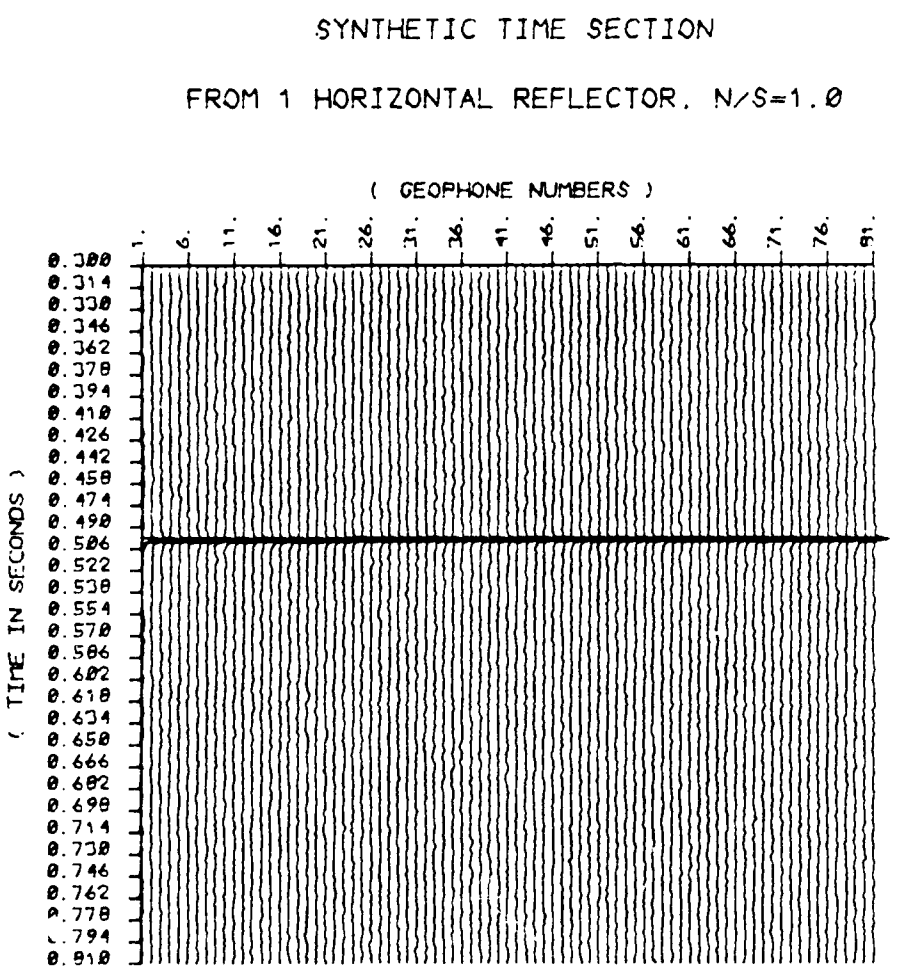

FIGURE IV.A3.1

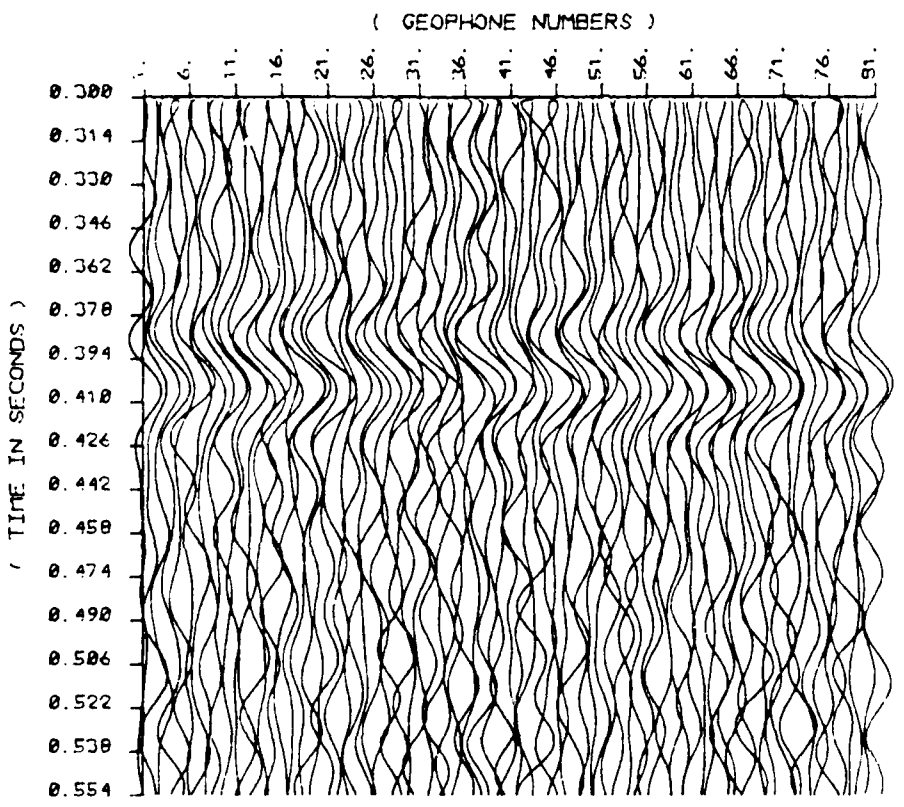

FIGURE IV.A3.2

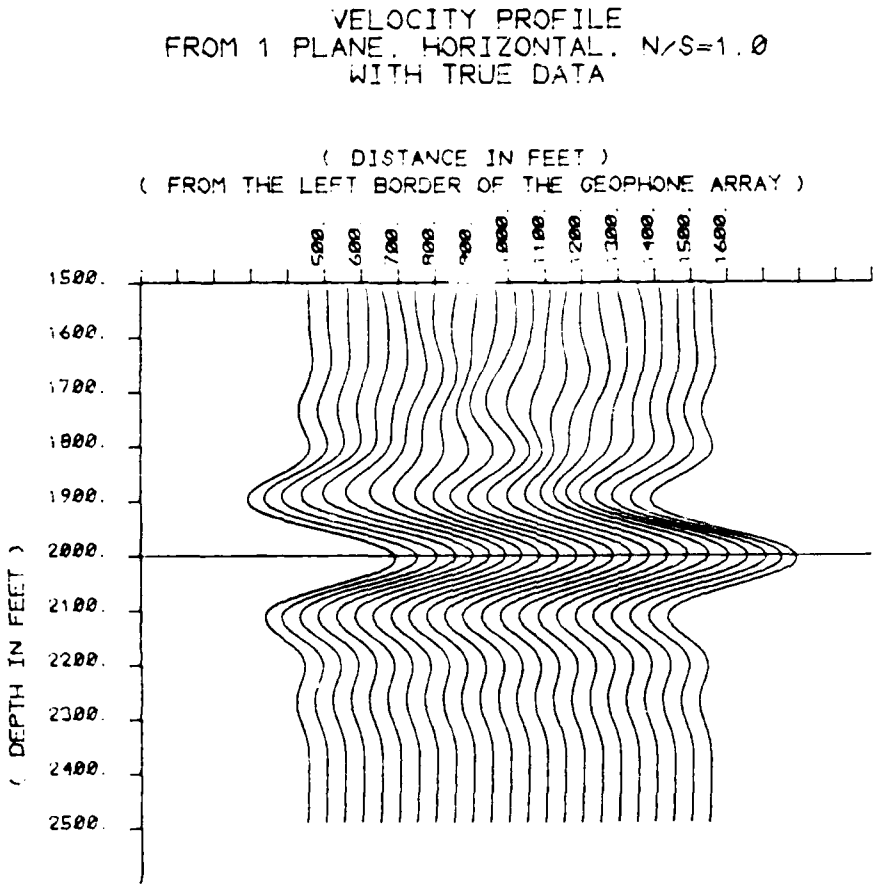

FIGURE IV.A3.3

AD-A154 776 QUALITATIVE ANALYSIS OF SIGN-BIT PROCESSING(U) COLORADO 2/2
SCHOOL OF MINES GOLDEN CENTER FOR WAVE PHENOMENA
I LEROUX 30 APR 85 CWP-028 N00014-84-K-0049

UNCLASSIFIED F/G 9/2 NL

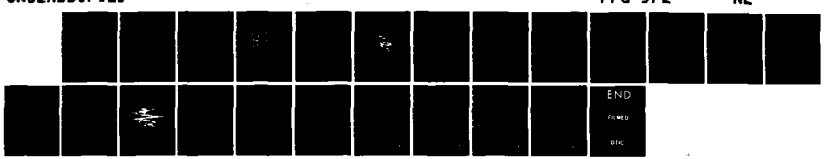

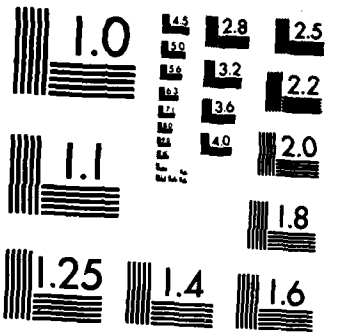

PROCESSED TIME SECTION
WITH SIGN-BIT AMPLITUDE DATA
FROM 1 PLANE. HORIZONTAL. N/S=1.0.

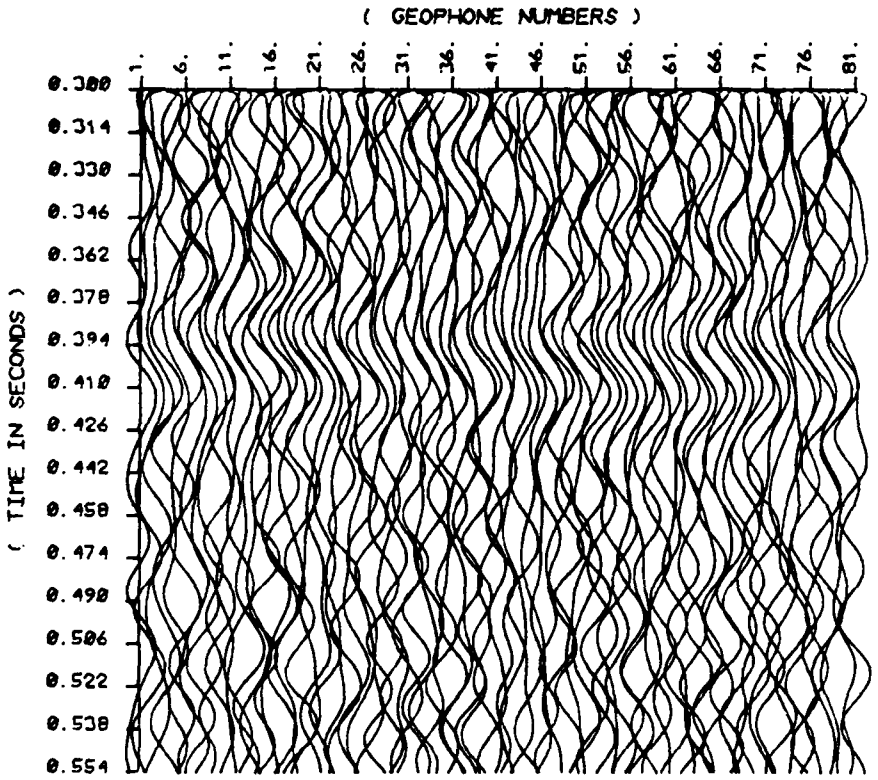

FIGURE IV.A3.4

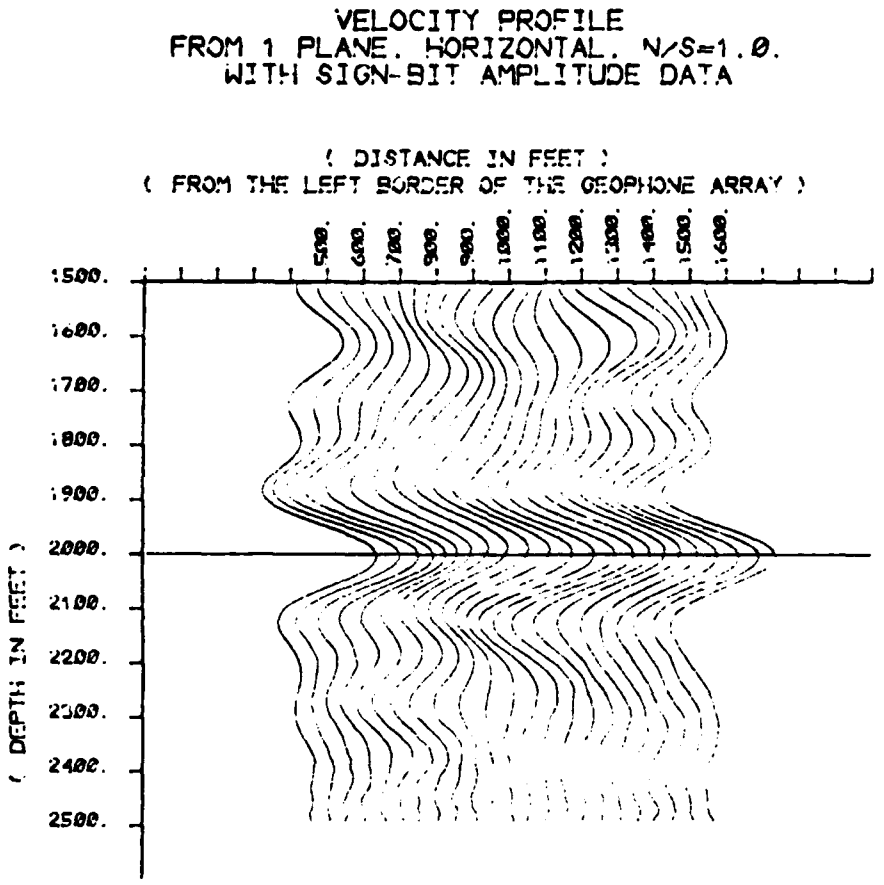

FIGURE IV.A3.5

SYNTHETIC TIME SECTION

FROM 1 HORIZONTAL REFLECTOR. N/S=25.6

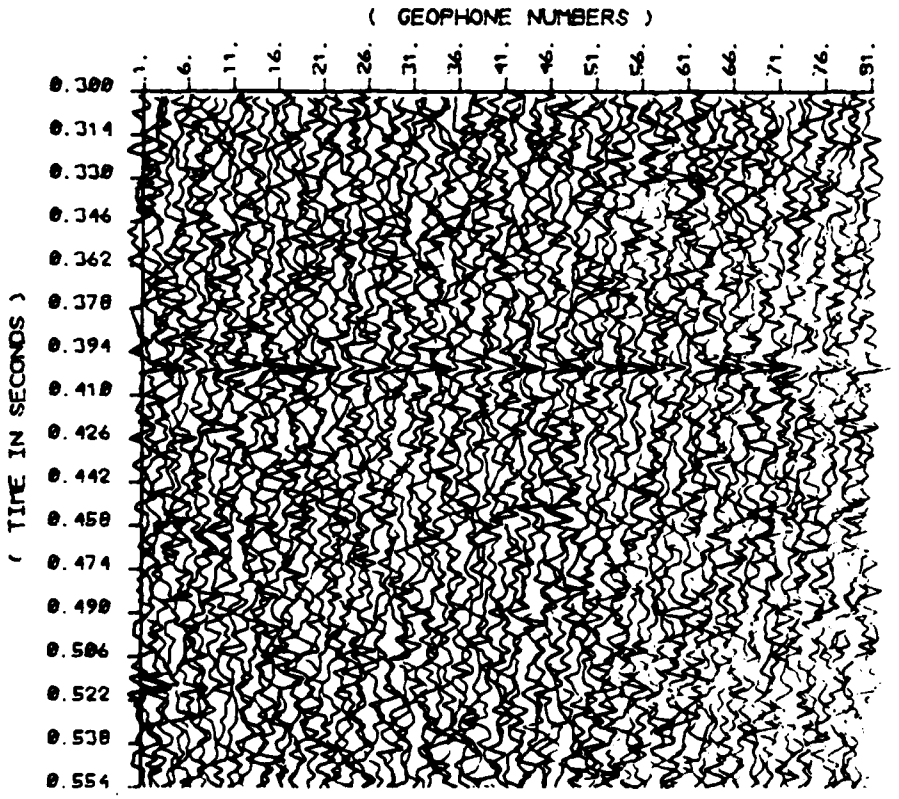

FIGURE IV.A4.1

PROCESSED TIME SECTION
WITH TRUE DATA
FROM 1 PLANE. HORIZONTAL. N/S=25.6

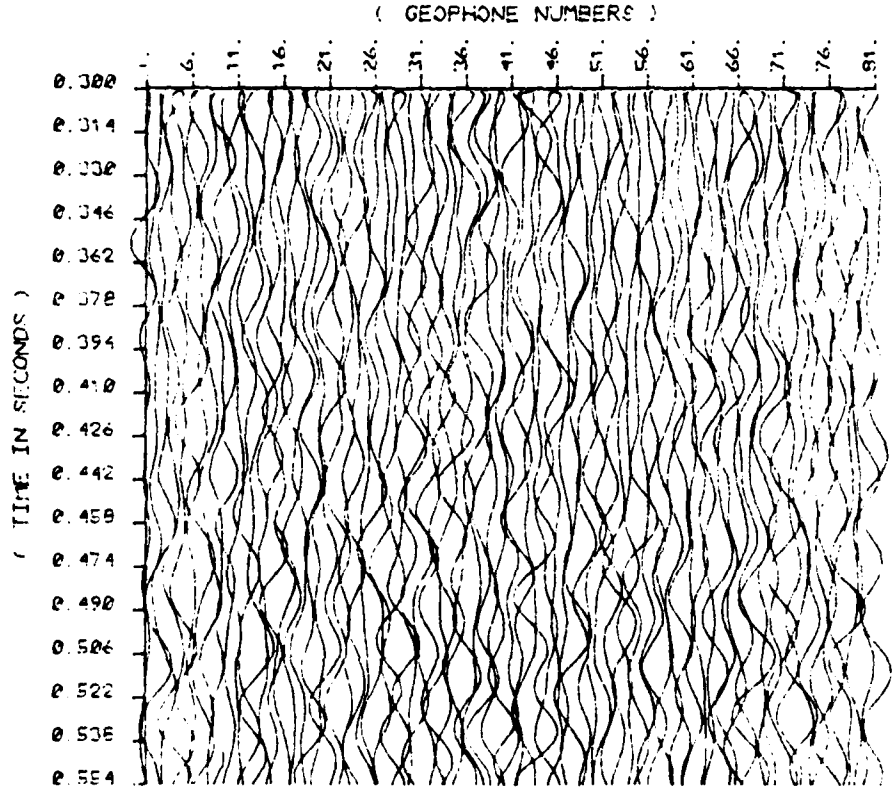

FIGURE IV.A4.2

VELOCITY PROFILE
WITH TRUE DATA
FROM 1 HORIZONTAL PLANE. N/S=25.6

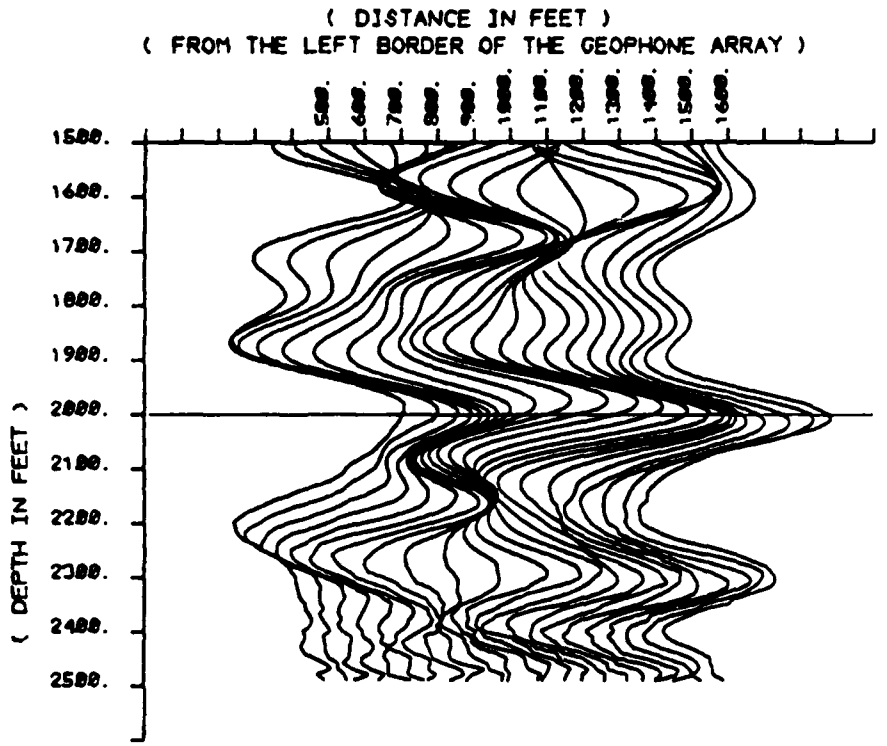

FIGURE IV.A4.3

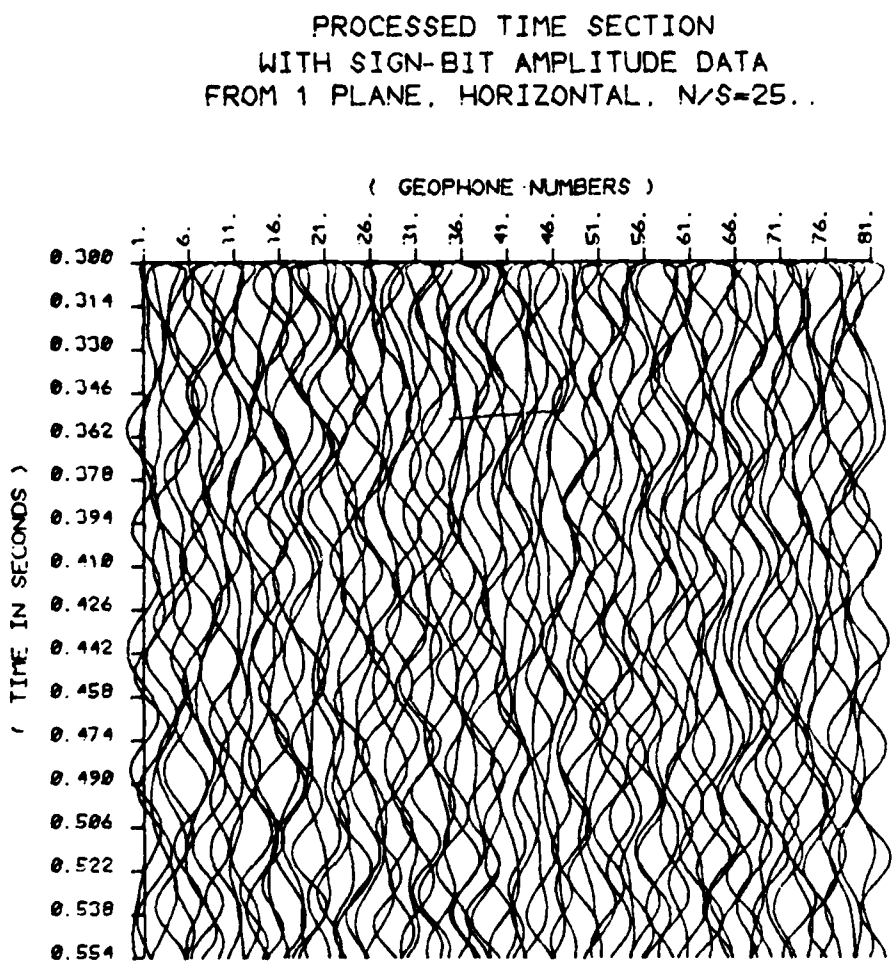

FIGURE IV.A4.4

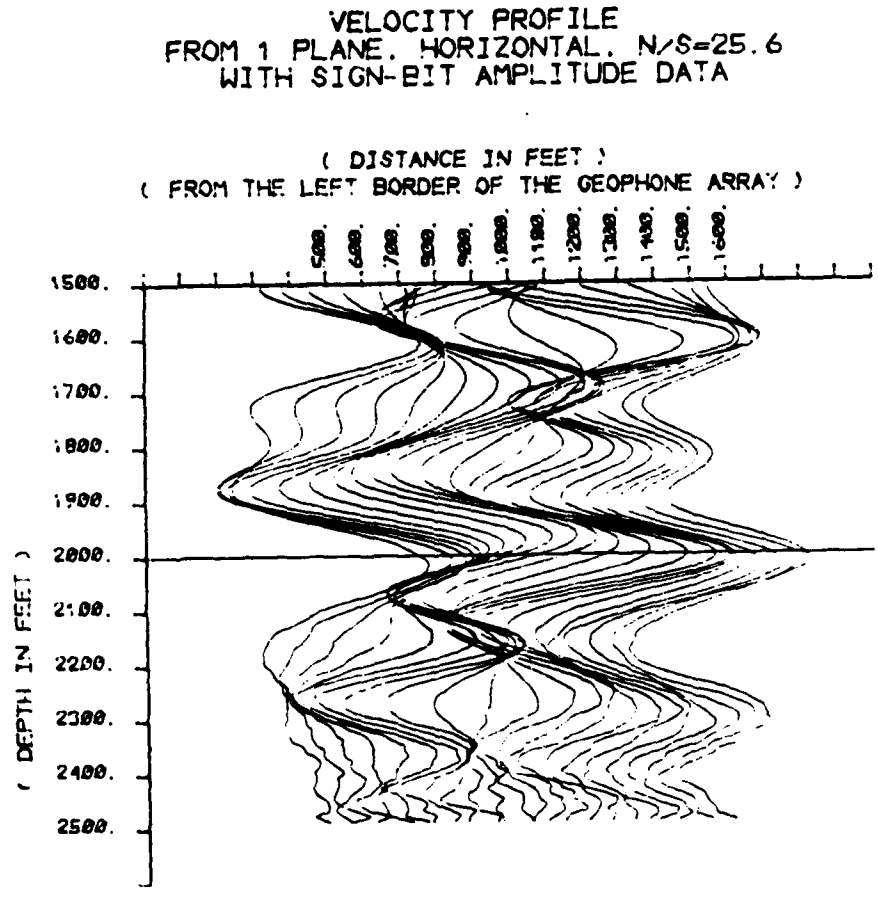

FIGURE IV.A4.5

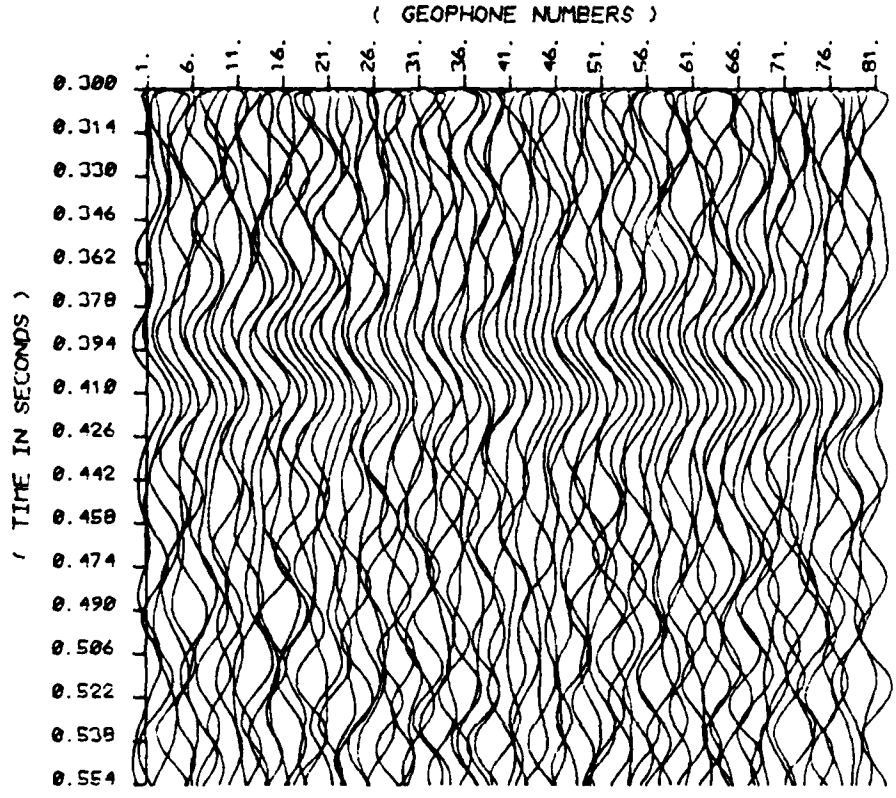
PROCESSED TIME SECTION
WITH THRESHOLD=0.05
FROM 1 PLANE. HORIZONTAL. N/S=0.5.
(GEOPHONE NUMBERS)
1.
6.
11.
16.
21.
26.
31.
36.
41.
46.
51.
56.
61.
66.
71.
76.
81.
(TIME IN SECONDS)
0.300
0.314
0.330
0.346
0.362
0.378
0.394
0.410
0.426
0.442
0.458
0.474
0.490
0.506
0.522
0.538
0.554

FIGURE IV.B.1

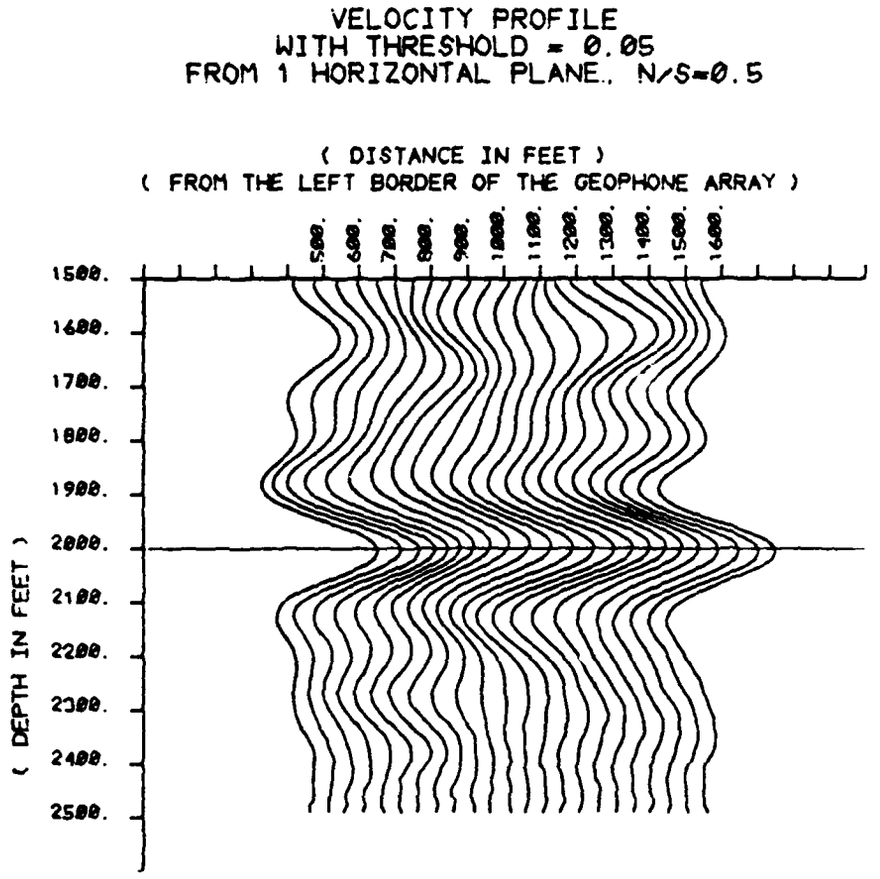
VELOCITY PROFILE
WITH THRESHOLD = 0.05
FROM 1 HORIZONTAL PLANE., N/S=0.5
(DISTANCE IN FEET)
(FROM THE LEFT BORDER OF THE GEOPHONE ARRAY)
500.
600.
700.
800.
900.
1000.
1100.
1200.
1300.
1400.
1500.
1600.
(DEPTH IN FEET)
1500.
1600.
1700.
1800.
1900.
2000.
2100.
2200.
2300.
2400.
2500.

FIGURE IV.B.2

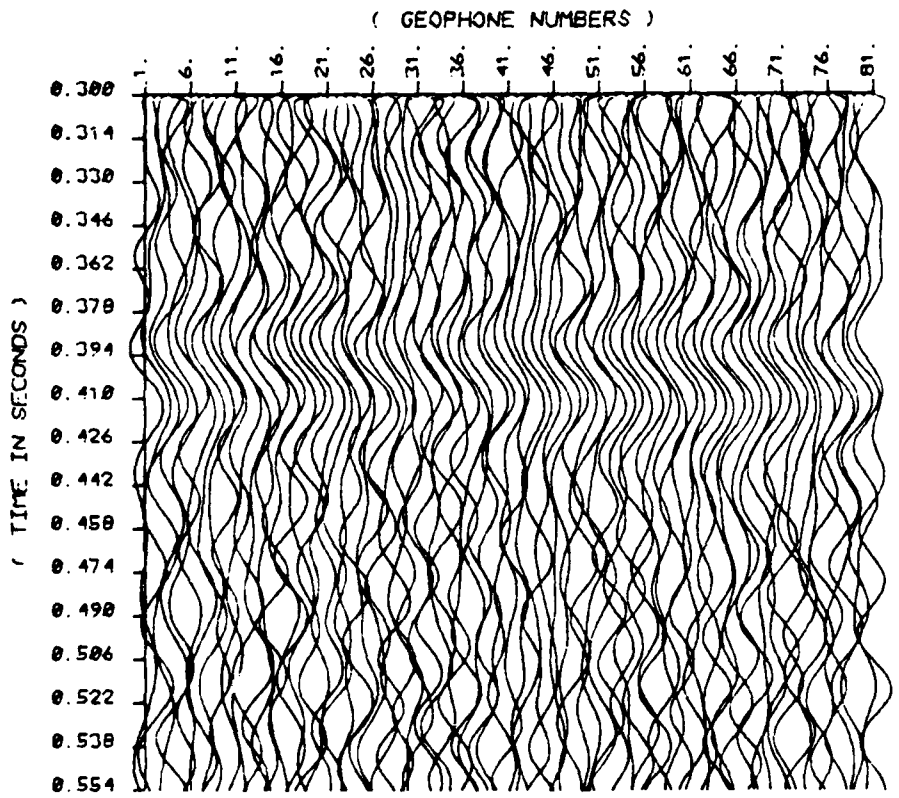
PROCESSED TIME SECTION
WITH THRESHOLD=0.10
FROM 1 PLANE. HORIZONTAL. N/S=0.5.
(GEOPHONE NUMBERS)
1.
6.
11.
16.
21.
26.
31.
36.
41.
46.
51.
56.
61.
66.
71.
76.
81.
(TIME IN SECONDS)
0.300
0.314
0.330
0.346
0.362
0.378
0.394
0.410
0.426
0.442
0.458
0.474
0.490
0.506
0.522
0.538
0.554

FIGURE IV.B.3

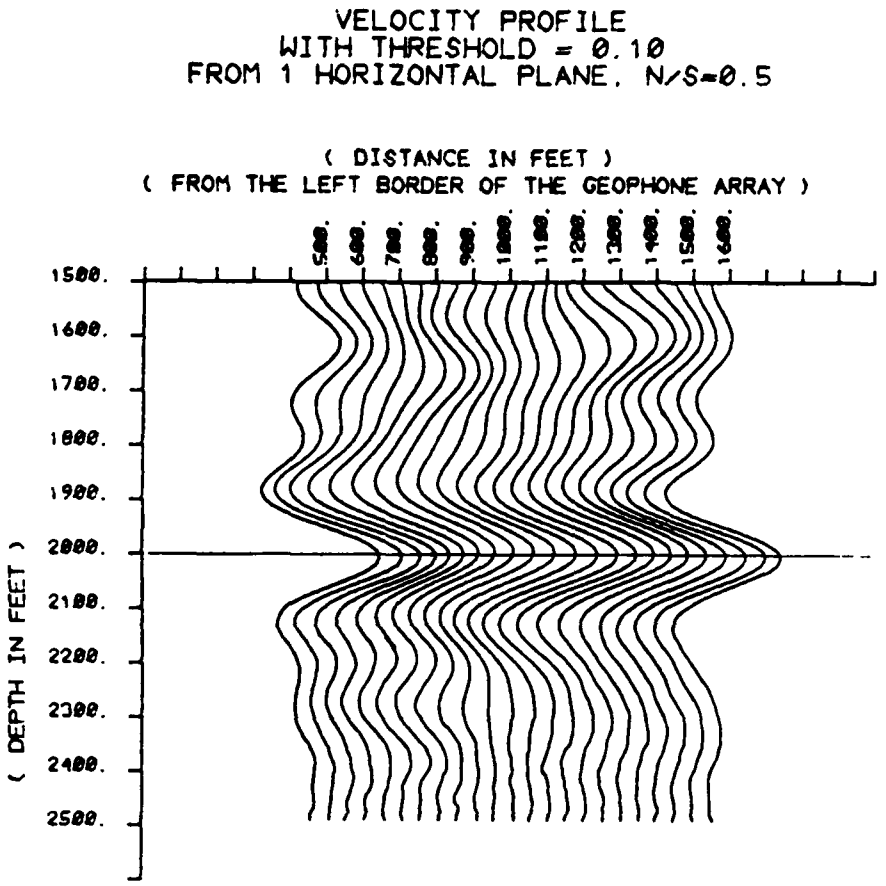
VELOCITY PROFILE
WITH THRESHOLD = 0.10
FROM 1 HORIZONTAL PLANE. N/S=0.5
(DISTANCE IN FEET)
(FROM THE LEFT BORDER OF THE GEOPHONE ARRAY)
(DEPTH IN FEET)
1500.
1600.
1700.
1800.
1900.
2000.
2100.
2200.
2300.
2400.
2500.

FIGURE IV.B.4

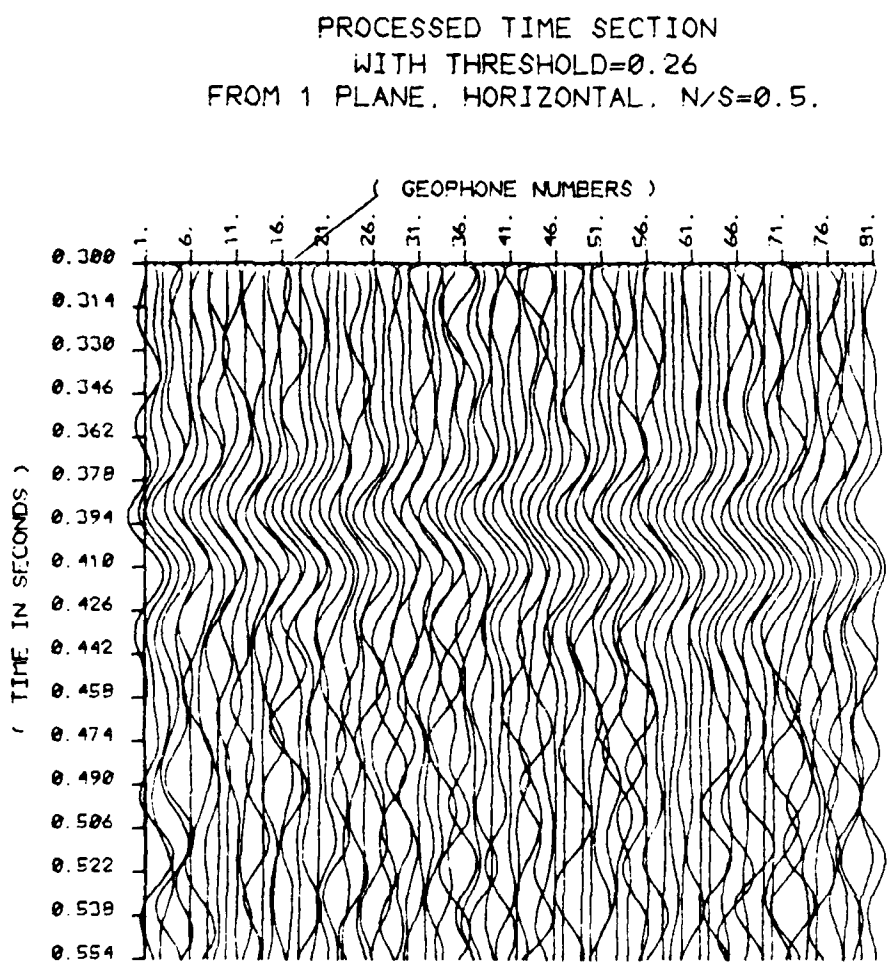
PROCESSED TIME SECTION
WITH THRESHOLD=0.26
FROM 1 PLANE. HORIZONTAL. N/S=0.5.
(GEOPHONE NUMBERS)
1.
6.
11.
16.
21.
26.
31.
36.
41.
46.
51.
56.
61.
66.
71.
76.
81.
(TIME IN SECONDS)
0.300
0.314
0.330
0.346
0.362
0.378
0.394
0.410
0.426
0.442
0.458
0.474
0.490
0.506
0.522
0.538
0.554

FIGURE IV.B.5

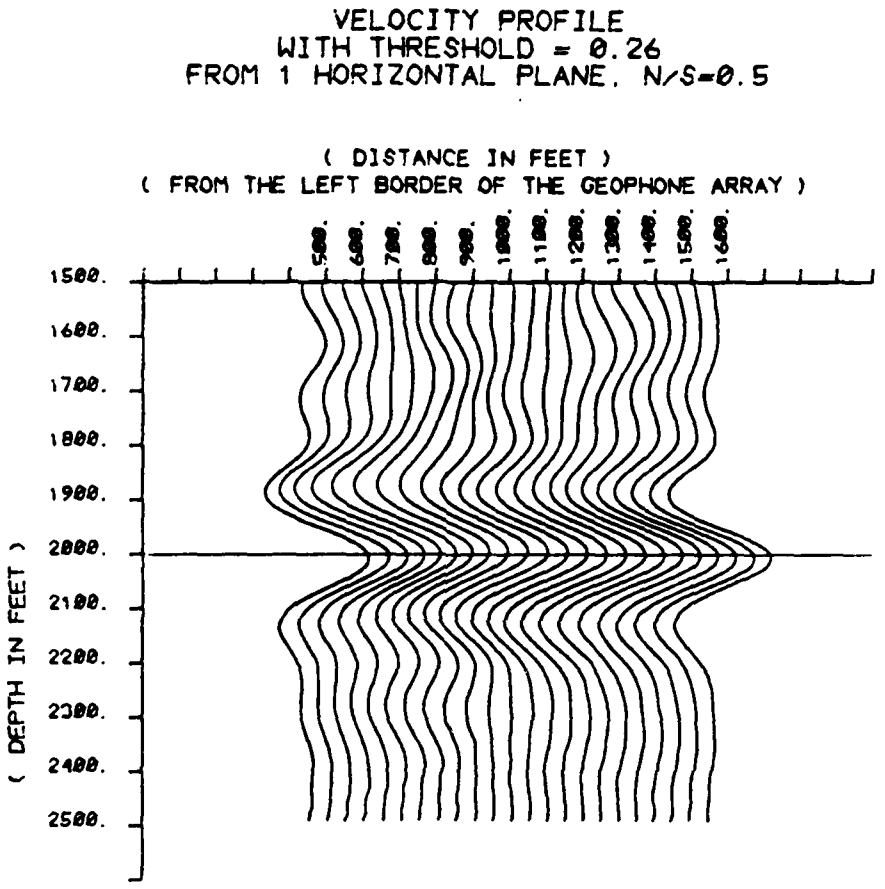
VELOCITY PROFILE
WITH THRESHOLD = 0.26
FROM 1 HORIZONTAL PLANE. N/S=0.5
(DISTANCE IN FEET)
(FROM THE LEFT BORDER OF THE GEOPHONE ARRAY)
500.
600.
700.
800.
900.
1000.
1100.
1200.
1300.
1400.
1500.
1600.
(DEPTH IN FEET)
1500.
1600.
1700.
1800.
1900.
2000.
2100.
2200.
2300.
2400.
2500.

FIGURE IV.B.6

PROCESSED TIME SECTION
WITH NOT FILTERED SIGN-BIT DATA
FROM 1 HORIZONTAL REFLECTOR. N/S=1.0.

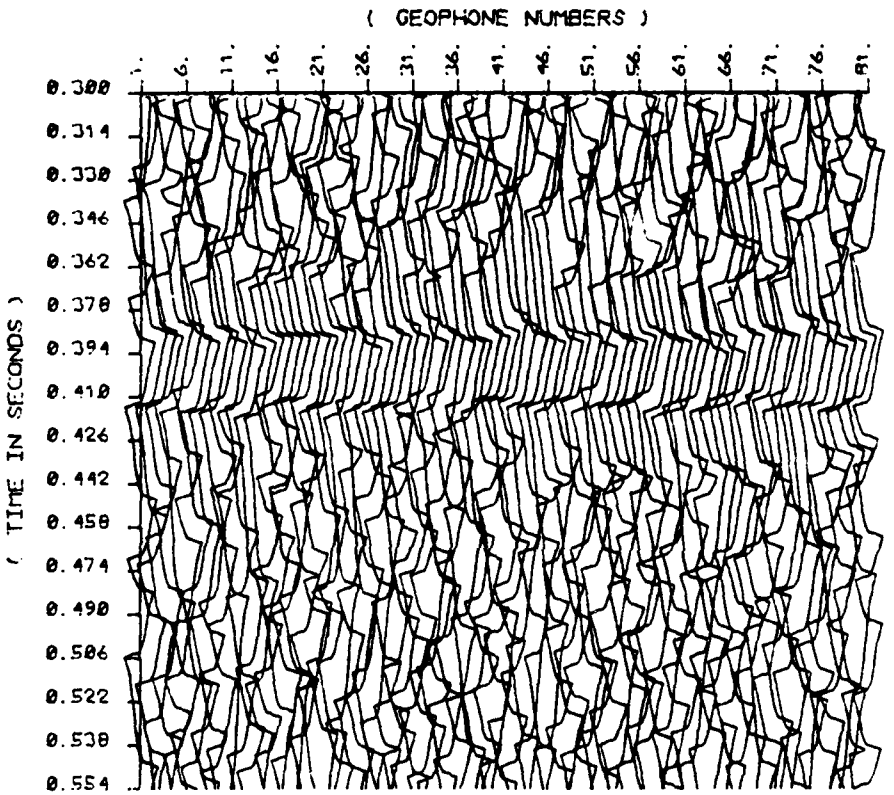

FIGURE IV.C.1

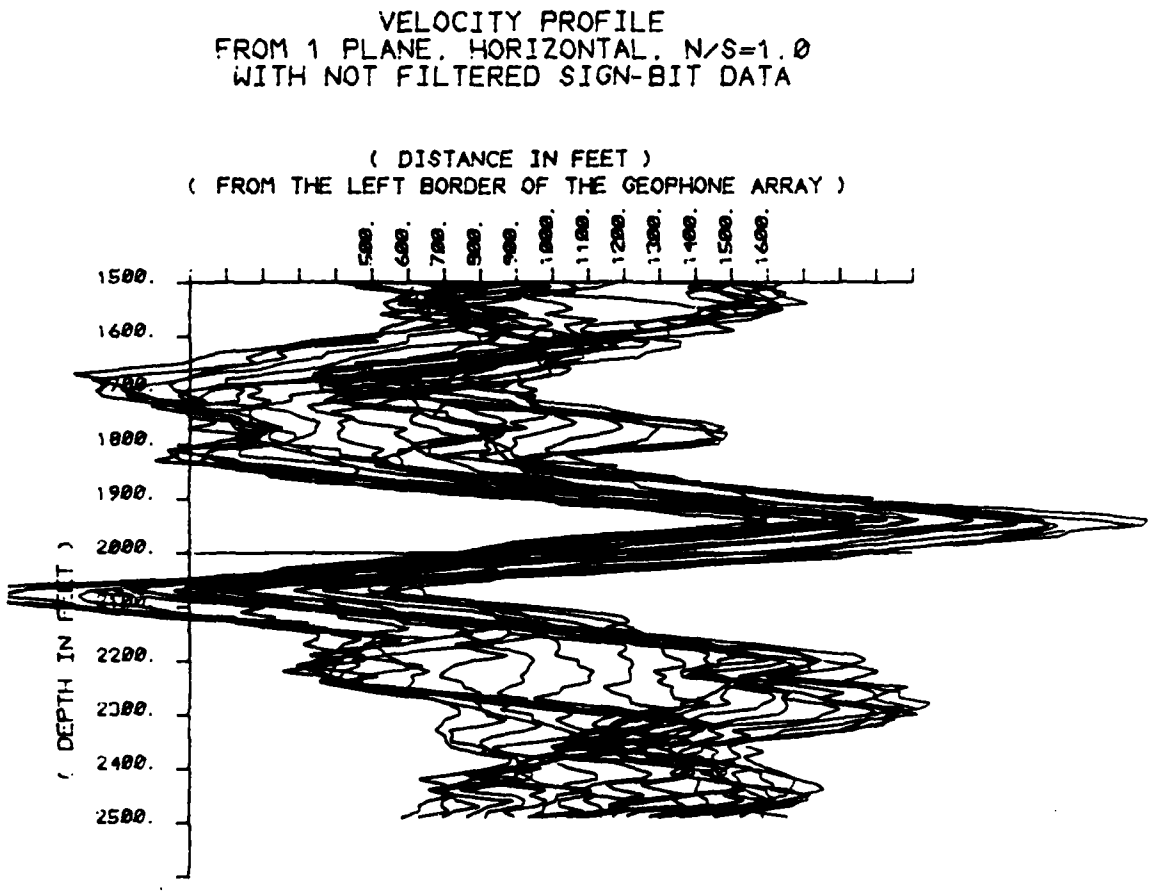
VELOCITY PROFILE
FROM 1 PLANE. HORIZONTAL. N/S=1.0
WITH NOT FILTERED SIGN-BIT DATA
(DISTANCE IN FEET)
(FROM THE LEFT BORDER OF THE GEOPHONE ARRAY)
1500.
1600.
1800.
1900.
2000.
2200.
2300.
2400.
2500.
(DEPTH IN FEET)

FIGURE IV.C.2

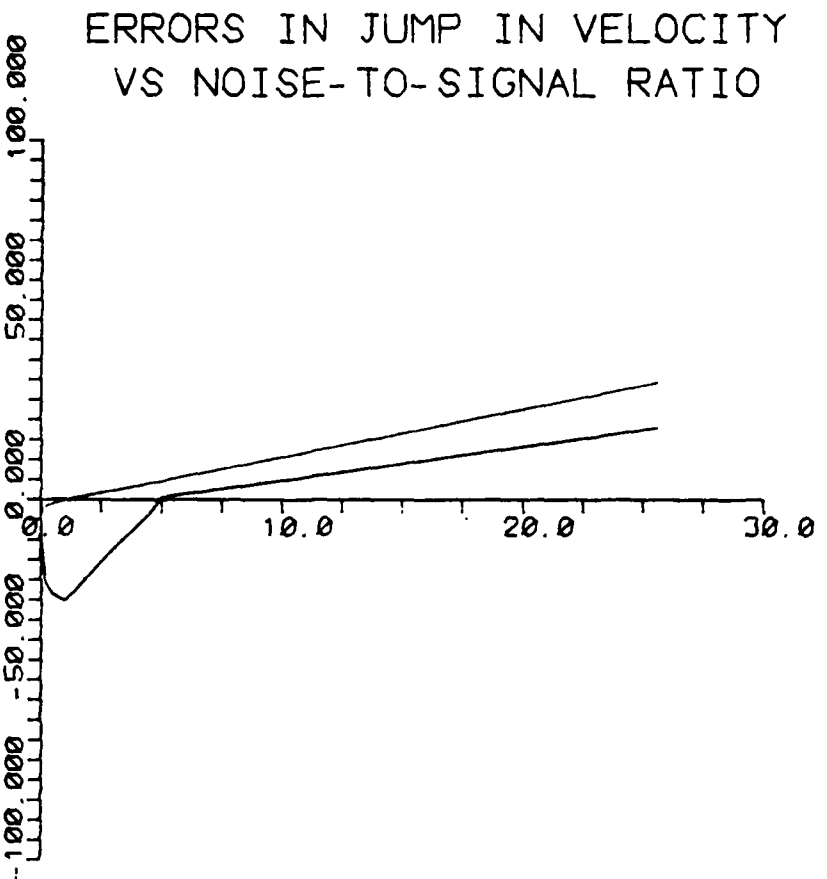

HIGHEST CURVE: FROM TRUE AMPLITUDE DATA PROCESSING.

LOWEST CURVE: FROM SIGN-BIT DATA PROCESSING.

FIGURE IV.C.3

VIII. APPENDICES

APPENDIX A

Data set for section III.A

TMIN	TMAX	DT	NPRT
6.0000E-01	1.0000E+00	4.0000E-03	120

FMING	FMIN1	FMAX1	FMAX0
2.000	6.000	15.000	20.000

DF= 1.953			
IFMIN0	IFMIN1	IFMAX1	IFMAX0
2	4	7	11

NG0	DXSI
91	25.0

SBAY
2000.0

C
5000.0

ZMIN	ZMAX	DZ :
1500.0	2500.0	10.0

XMIN	XMAX	DX :
450.0	1550.0	50.0

NZ	NX :
101	23

NRSPUR
21

MKPRNT	MKTAPE	MKPLOT	MKPIL :
T	T	F	T

[illegible]	NPLY	NOISIG	
0.00000	1	0.0000	

IPLY	ZS	CS	
1	2000.0	5000.0	
	9999999.0	5000.0	

PHAID	PNYC	PPHAS	PMESH :
0.82	12.50	1.88	0.40

APPENDIX B

Data set for section III.C

TMIN	TMAX	DT	NFET
6.000E-01	1.000E+00	4.000E-03	128

FMIN0	FMIN1	FMAX1	FMAX0
2.000	6.000	12.000	20.000

IFMIN0	IFMIN1	IFMAX1	IFMAX0
2	4	7	11

NSEG	DASI
91	35.0

SPAN
2000.0

C
5000.0

ZMIN	ZMAX	DZ :
1500.0	2500.0	10.0

XMIN	XMAX	DX :
450.0	1550.0	50.0

NZ	NY :
101	23

NGROUP
21

MKPRT :	MKTAPE	MKPLOT	MKFIL :
T	F	F	T

THETS	NPLN	NOISIG
0.0000	2	0.0000

IPLN	ZS	CS
1	1700.0	5000.0
2	2300.0	5500.0
3	9999999.9	6000.0

PBAND	PAYC	PPHASE	PMESH :
0.82	12.50	1.98	0.40

APPENDIX C

Data set for section III.E

WITH A REFLECTOR which is an arc of circle
with radius : 3000.00

TMIN	TMAX	DT	NFRT
3.000E-01	7.000E-01	4.000E-03	12
FMIN0	FMIN1	FMAX1	FMAX0
3.000	6.000	12.000	20.000
DF= 1.953			
IFMIN0	IFMIN1	IFMAX1	IFMAX0
3	4	7	11
NGEO	DXSI		
81	25.0		
SPAN			
2000.0			
C			
5000.0			
ZMIN	ZMAX	DZ :	
750.0	1750.0	20.0	
XMIN	XMAX	DX :	
450.0	1550.0	50.0	
NZ	NX :		
51	23		
NGROUP			
21			
MKPRNT	MKTAPE	MKPLOT	MKFIL :
T	F	F	T
THETS	NPLN	NOISIG	
0.0000	1	0.0000	
IPLN	ZS	CS	
1	1000.0	5000.0	
2	9999999.0	5500.0	

APPENDIX D

Data set for section III.D

TIME	TMAX	DT	NPRT
6.000E-01	1.000E+00	4.000E-03	12
FMIN	FMIN1	FMAX1	FMAX0
0.000	6.000	12.000	20.000
IFMIN0	IFMIN1 1.953	IFMAX1	IFMAX0
	2		11
NG	DXSI		
21	20.0		
SFAC			
2000.0			
5000.0			
ZMIN	ZMAX	DZ :	
1500.0	2500.0	20.0	
XMIN	XMAX	DX :	
450.0	1550.0	50.0	
NZ	NY :		
21	23		
NGRID			
21			
MPRINT	MTAPE	MKPLOT	MYPIL :
1	5	F	T
THETA	NPLT	NDISIC	
10.0000	1	0.0000	
IPLT	ZS	CS	
1	1900.0	5000.0	
2	2400.0	5500.0	
3	9999999.0	5700.0	
DLIMD	PMAG	PPHASE	PMTSW :
0.25	12.50	1.85	0.40

END

FILMED

7-85

DTIC